Balancing Utility and Privacy: Dynamically Private SGD with Random Projection

Anonymous authors
Paper under double-blind review

Abstract

Stochastic optimization is a pivotal enabler in modern machine learning, producing effective models for various tasks. However, several existing works have shown that model parameters and gradient information are susceptible to privacy leakage. Although Differentially Private SGD (DPSGD) addresses privacy concerns, its static noise mechanism impacts the error bounds for model performance. Additionally, with the exponential increase in model parameters, efficient learning of these models using stochastic optimizers has become more challenging. To address these concerns, we introduce the Dynamically Differentially Private Projected SGD (D2P2-SGD) optimizer. In D2P2-SGD, we combine two important ideas: (i) dynamic differential privacy (DDP) with automatic gradient clipping and (ii) random projection with SGD, allowing dynamic adjustment of the tradeoff between utility and privacy of the model. It exhibits provably sub-linear convergence rates across different objective functions, matching the best available rate. The theoretical analysis further suggests that DDP leads to better utility at the cost of privacy, while random projection enables more efficient model learning. Extensive experiments across diverse datasets show that D2P2-SGD remarkably enhances accuracy while maintaining privacy. Our code is available here.

1 Introduction

Deep learning models Thirunavukarasu et al. (2023); Menghani (2023), enabled by stochastic optimization techniques, have achieved remarkable success in many fundamental machine learning tasks. Though these models empirically show incredibly appealing capabilities, there are critical concerns regarding the privacy of these models. In numerous applications, such as healthcare Chen et al. (2021) and finance Goodell et al. (2021), training datasets often contain highly sensitive information that must remain confidential. However, due to the widespread use of deep learning models, their rich representations can possibly disclose private information under privacy attacks, as demonstrated in the prior works Zhao et al. (2020); Wang et al. (2022a). Additionally, as the number of model parameters increases exponentially, it is unclear to us how privacy and model performance affect each other as the learning becomes more computationally complex.

Related Works. To mitigate these privacy concerns, *differential privacy* (DP) Dwork (2006; 2008) was introduced, and it has gained considerable attention Ji et al. (2014); Blanco-Justicia et al. (2022) to provide principled and rigorous privacy guarantees. Intuitively speaking, DP is a mechanism to ensure that all data samples have no significant impact on the ultimate trained model. Differentially private SGD (DPSGD) Abadi et al. (2016); Bassily et al. (2014) is one of the most acknowledged methods to solve the private empirical risk minimization (ERM) problems. Specifically, it perturbs each gradient update with a static random noise vector (with the same dimension as that of the gradient) sampled from a distribution. The dimension of the noise vector is typically the same as that of the gradient, which could be extremely large and problematic. More advanced variants on top of DPSGD have also been developed to consider other key issues, such as communication-efficient distributed setting Agarwal et al. (2018); Li & Chi (2025), non-smooth losses Wang et al. (2022b), uniform Lipschitz condition Das et al. (2023), and compilation and vectorization Subramani et al. (2021). Using the perturbed gradient updates, we can compute the tradeoff between the utility and privacy of the model. This tradeoff can be adjusted via a noise mechanism, typically sampled from a *static* distribution with properly chosen yet fixed variance. While this approach is technically

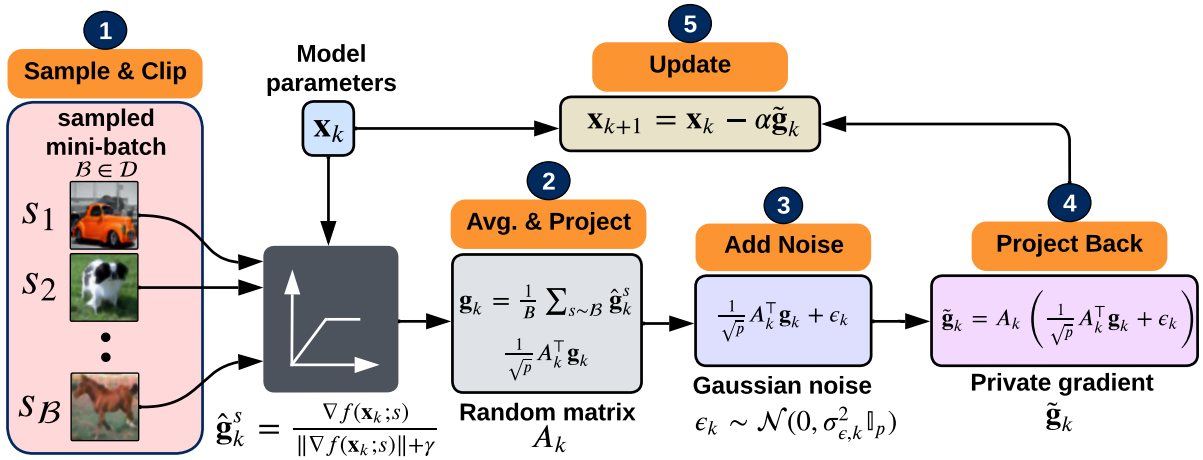

Figure 1: D2P2-SGD method involves five steps. For more technical details, please see Algorithm 1.

simple and provably effective, the noise variance significantly impacts the ultimate error bound. A challenging issue that remains in various private machine learning tasks is how to achieve a desirable tradeoff between privacy and utility, which becomes particularly important in large-scale deep learning models Flemings et al. (2024); Mattern et al. (2022). Recent work Du et al. (2021) proposed a dynamic DP mechanism to adjust the tradeoff on the fly, reducing the model performance loss gap at the cost of increased privacy loss. Further, the dimension of the noise vector is typically the same as that of the gradient, which could be extremely large to cause intensive computational complexity. This issue motivates us to seek out an approach that assists in reducing the complexity while maintaining privacy. Inspired by the work Blocki et al. (2012), we pay attention to model compression techniques as follows. Though numerous prior works have extensively studied the tradeoff, most attempts rarely investigated how to dynamically adjust it along the optimization using a dynamic DP mechanism.

Model compression Buciluǎ et al. (2006); Choudhary et al. (2020) has been utilized to reduce the computational complexity, including quantization Chmiel et al. (2020), regularization Moradi et al. (2020); Orvieto et al. (2023), and projection Gu et al. (2023); Tsfadia (2024). Though these methods aim to reduce computational complexity, their technical details can differ significantly depending on the specific focus. For example, in Gu et al. (2023), the authors used projection to identify the dominating gradient subspace, which facilitated improving model accuracy without changing the dimension of model parameters. This is akin to L1-norm regularization Xu et al. (2008), which forces certain model parameters to become exactly zero. Although model compression offers promising performance, it comes at the expense of possible accuracy reduction and sophisticated compression techniques, necessitating an effective optimizer that can balance the dynamic trade-off between privacy and utility. Additionally, the dimension of the noise vector is typically the same as that of the gradient, which could be extremely large and problematic. Consequently, effective approaches should be studied further to look into the tradeoff between privacy and utility while lowering the dimension of the additive noise. Additional related works are provided in Appendix A.1.

In this work, we highlight the need for an effective optimizer to balance among complexity, privacy and utility; answering the critical question:

Can we design an adaptive differentially private optimizer to allow a small model performance reduction gap and maintain privacy?

Contributions. In this work, we answer the above question affirmatively. Specifically, we propose a novel stochastic optimizer termed Dynamically Differentially Private Projected SGD (D2P2-SGD) (as shown in Figure 1), which, for the first time, integrates the dynamic DP mechanism with automatic gradient clipping and random projection for optimization. The dynamic DP mechanism involves an isotropic Gaussian

distribution with a properly chosen *time-varying* variance that decreases along with the iterations, reducing noise effects as privacy loss increases. To further warrant differential privacy and bound the influence of each individual example on the stochastic gradient, we resort to a recently developed automatic gradient clipping mechanism Bu et al. (2024). This is different from the traditional clipping method Abadi et al. (2016), where an upper bound is imposed for gradients. Additionally, the stochastic gradient is projected into a lower-dimensional space, reducing the dimension of additive noise and mitigating the increase in privacy loss. Concretely, the main contributions are as follows:

1. We introduce a novel DP optimizer, D2P2-SGD, that employs a dynamic DP mechanism with a *time-varying* noise variance and random projection. This approach minimizes model performance loss and reduces the dimensionality of noise vectors added to the stochastic gradients. Additionally, the per-sample gradient normalization serves as an automatic gradient clipping mechanism to regulate the influence of individual examples on the stochastic gradient.

2. Theoretically, we prove that D2P2-SGD achieves sub-linear convergence rates for both generally convex and non-convex functions, matching the best available convergence rate of regular SGD. The results for the dynamic DP mechanism can immediately degenerate to those for static scenarios, revealing the consolidation among complexity, utility, and privacy.

3. Extensive evaluations on a wide spectrum of datasets confirm that D2P2-SGD significantly improves model accuracy compared to baseline methods.

In this paper, our approach prioritizes theoretical exploration over scalability to larger datasets and models, including transformers and large language models Kasneci et al. (2023). While progress has been made in this domain Yu et al. (2021), designing a differentially private optimizer for such models remains a significant challenge and is deferred to future work.

Table 1: Comparison among different methods.

Method	**Noise**	**Compression**	**Rate**
DPSGD[1]	Static	N	$\mathcal{O}(\frac{1}{\sqrt{K}})$
PDP-SGD[2]	Static	Y	$\mathcal{O}(\frac{1}{\sqrt{K}})$
DPKD[3]	Static	N	N/A
Anti-PGD[4]	Static	N	$\mathcal{O}(\frac{1}{\sqrt{K}})$
Dynamic DPSGD[5]	Dynamic	N	$\mathcal{O}(\frac{1}{\sqrt{K}})$
PrivSGD[6]	Static	Y	$\mathcal{O}(\frac{1}{\sqrt{K}})$
RQP-SGD[7]	Static	Y	$\mathcal{O}(\frac{1}{\sqrt{K}})$
ADP-SGD[8]	Static	N	$\mathcal{O}(\frac{1}{\sqrt{K}})$
PORTER[9]	Static	Y	$\mathcal{O}(\frac{1}{\sqrt{K}})$
D2P2-SGD (Convex)	Dynamic	Y	$\mathcal{O}(\frac{1}{\sqrt{K}} + \frac{\ln K}{K^{1.5}})$
D2P2-SGD (Non-convex)	Dynamic	Y	$\mathcal{O}(\frac{1}{\sqrt{K}} + \frac{\ln K}{K^{1.5}})$

1: Bassily et al. (2014); 2: Zhou et al. (2020); 3: Mireshghallah et al. (2022); 4: Koloskova et al. (2023b); 5: Du et al. (2021); 6: Kasiviswanathan (2021); 7: Feng & Venkitasubramaniam (2024); 8: Bu et al. (2024); 9: Li & Chi (2025); N: no; Y: yes

2 Problem Formulation and Preliminaries

Given a private dataset $\mathcal{D} = \{s_1, s_2, ..., s_n\}$ sampled in an i.i.d. manner from a distribution $\mathcal{P}$ such that we want to solve the empirical risk minimization (ERM) problem subject to differential privacy:

$$\min_{\mathbf{x}} f(\mathbf{x}) = \frac{1}{n} \sum_{s \in \mathcal{D}} f(\mathbf{x}, s), \tag{1}$$

where $\mathbf{x} \in \mathbb{R}^d$ and $f(\cdot, \cdot)$ is the loss for a single sample. We aim to optimize Eq. 1 with a gradient-based algorithm in a differentially private manner. We denote by $\mathbf{x}_k$ the model parameters' iterate and $\mathbf{g}_k$ the mini-batch gradient at each time step k. Throughout the analysis, we assume that $\mathbf{g}_k$ is the unbiased estimate of $\nabla f(\mathbf{x}_k)$, i.e., $\nabla f(\mathbf{x}_k) = \mathbb{E}(\mathbf{g}_k)$. In this context, we resort to *gradient clipping mechanism* to constrain the magnitude of the stochastic gradient $\mathbf{g}_k$. To provide the guarantee of differential privacy, it requires bounding the influence of each individual example on $\mathbf{g}_k$. A fairly popular clipping operation Abadi et al. (2016) applied to vector $\mathbf{v} \in \mathbb{R}^d$ is as: $\text{clip}(\mathbf{v}, G) = \min\{1, \frac{G}{\|\mathbf{v}\|}\} \cdot \mathbf{v}$, where $G > 0$, $\|\cdot\|$ is the l_2 norm. However, when applying this to the stochastic gradient, such an operation will inevitably result in a "lazy region" issue, particularly if $\|\mathbf{v}\| > G$. This means the parameters will not be updated even if the true gradients are non-zero. Therefore, to mitigate this issue, we leverage a recently developed *per-sample gradient normalization* Bu et al. (2024) as an automatic clipping mechanism described as: $\text{clip}(\mathbf{v}, G, \gamma) = \frac{G}{\|\mathbf{v}\| + \gamma}$, where γ is a positive stability constant, which is practically small. Additionally, the authors even showed that any constant choice G is equivalent to choosing $G = 1$. In this work, for the algorithmic framework, we follow their setup to directly set $G = 1$, while still keeping G in the theoretical analysis, particularly for the generally convex objective, which is missing in Bu et al. (2024). Additionally, we will reveal that for any $\gamma > 0$, when the objective is non-convex, the gradient norm will converge to a neighborhood of the optimal solution affected by γ. To characterize the analysis for the proposed scheme, we introduce the necessary background and preliminary knowledge in the sequel, starting with the standard definition of differential privacy.

Definition 1. *(ε-Differential Privacy Dwork (2006)) A randomized algorithm $\mathcal{M}$ is ε-differentially private if for any pair of datasets $\mathcal{D}, \mathcal{D}'$ differ in exactly one data point and for all events $\mathcal{Y} \subseteq Range(\mathcal{M})$ in the output range of $\mathcal{M}$, we have $Pr\{\mathcal{M}(\mathcal{D} \in \mathcal{Y})\} \leq \exp(\varepsilon) Pr\{\mathcal{M}(\mathcal{D}' \in \mathcal{Y})\}$, where the probability is taken over the randomness of $\mathcal{M}$.*

$Range(\mathcal{M})$ refers to the set of all possible outcomes of $\mathcal{M}$. Technically speaking, the set $\mathcal{Y}$ in Definition 1 must be measurable. This definition implies that the probability of observing a specific output on any two neighboring datasets can differ by at most a multiplicative factor of $\exp(\varepsilon)$. Intuitively, a sufficiently small ε value suggests that either including or excluding a single data point from the dataset does not likely affect the output. Hence, an adversary only accessing the output of $\mathcal{M}$ makes it difficult to infer whether any data point is present in the dataset. The parameter ε is called *privacy budget* and its practical selection varies significantly, depending on different scenarios Ponomareva et al. (2023). However, a relaxation of ε-DP in Definition 1 has been used more commonly instead for attaining better utility and easier privacy accounting for composing multiple DP mechanisms, which leads to the (ε, δ)-DP mechanism defined as follows.

Definition 2. *((ε, δ)-differential privacy Dwork (2006)) A randomized algorithm $\mathcal{M}$ is (ε, δ)-differentially private if for any two neighboring datasets $\mathcal{D}, \mathcal{D}'$ and for all events $\mathcal{Y} \subseteq Range(\mathcal{M})$ in the output range of $\mathcal{M}$, we have $Pr\{\mathcal{M}(\mathcal{D} \in \mathcal{Y})\} \leq \exp(\varepsilon) Pr\{\mathcal{M}(\mathcal{D}' \in \mathcal{Y})\} + \delta$, where the probability is taken over the randomness of $\mathcal{M}$.*

Here, it can be observed that δ controls the strength of the relaxation, compared to Definition 1, with smaller values leading to stronger privacy guarantees. A generally recommended δ value in the literature is to choose $\delta \ll \frac{1}{n}$ Ponomareva et al. (2023). In our analysis, we will establish the privacy guarantee for the proposed algorithm presented in the next section. Before that, we present preliminaries on random projection and formally define the projection matrix.

Random projection (RP) Achlioptas (2001) is an effectively fundamental tool that has been used in numerous applications to analyze datasets and then characterize their major features. It projects data points to random directions that are independent of the dataset, which renders simpler and computationally faster trends than

classical methods such as singular value decomposition (SVD). RP is based upon the Johnson-Lindenstrauss lemma Larsen & Nelson (2017) as follows.

Definition 3. *(Johnson-Lindenstrauss Lemma Larsen & Nelson (2017)) For any $0 < \zeta < 1$, a set $\mathcal{S}$ of m points in $\mathbb{R}^d$, and an integer $p > 8(\ln m)/\zeta^2$, there exists a linear map $h : \mathbb{R}^d \to \mathbb{R}^p$, such that $(1-\zeta)\|u-v\|^2 \leq \|h(u)-h(v)\|^2 \leq (1+\zeta)\|u-v\|^2$, for all $u, v \in \mathcal{S}$.*

Johnson-Lindenstrauss lemma states that a set of points in a high-dimensional space can be projected into a lower-dimensional subspace such that their relative distances are nearly preserved. Inspired by this, we adapt random projection techniques to model parameters or gradients Kasiviswanathan (2021) by projecting the counterpart from a high-dimensional space to its corresponding subspace, which facilitates efficient updates. Note also that the lower dimension subspace is selected randomly based on some distribution. According to Definition 3, we observe that the core to the Johnson-Lindenstrauss Lemma is the linear map h, which can be obtained through the following definition.

Definition 4. *Let A be a random matrix of order $d \times p$, i.e., $A_{ij} \sim \mathcal{N}(0,1)$ and o be any fixed vector in $\mathbb{R}^d$. Define $r = \frac{1}{\sqrt{p}} A^\top o$. Thus, $r \in \mathbb{R}^p$ and $r_i = \frac{1}{\sqrt{p}} \sum_j A_{ij} o_j$.*

We notice that each element of A is sampled from the same normal distribution $\mathcal{N}(0,1)$, while we use a slightly different variance, σ_A^2 instead of 1, in our theoretical analysis for a more generic purpose.

3 Algorithm and Main Results

3.1 Algorithmic Frameworks

D2P2-SGD is shown in Algorithm 1. Line 5 states the key gradient clipping operation to control the influence of the gradient magnitude. Compared to the clipping mechanism applied in Abadi et al. (2016), we do not need to tune the clipping threshold. In Line 7, a mini-batch stochastic gradient is calculated after the per-sample gradient clipping. In Line 9, the stochastic gradient $\mathbf{g}_k$ is projected to the lower-dimensional space $\mathbb{R}^p$ by using A_k, which is followed by adding the noise sampled from a Gaussian distribution with time-varying distribution $\sigma_{\epsilon,k}^2 \mathbb{I}_p$, where $\sigma_{\epsilon,k} = \frac{\sigma_\epsilon}{\sqrt{k}}$. With this, ϵ_k is *independent* of a high dimension d, but dependent on a lower dimension $p \ll d$, which fundamentally reduces the noise. The fact that we resort to the decay of $\frac{1}{\sqrt{k}}$ for the variance is motivated by the same setup to the learning rate in stochastic optimizers Bottou et al. (2018), which manipulates the tradeoff between the convergence speed and optimality. Analogously, $\sigma_{\epsilon,k}^2$ controls the impact of the noise mechanism on the tradeoff between privacy and utility in different phases of the optimization. Since the update for $\mathbf{x}_k$ is operated in the original dimension $\mathbb{R}^d$, we multiply the projected stochastic gradient by A_k to project it back to the original one. It is noted that such an implementation will cause projection errors that impact the error bound (which will be observed in the theoretical analysis). However, similar to Wang et al. (2019b), D2P2-SGD implies more efficient model learning as it has now focused primarily on the subspace in $\mathbb{R}^d$ instead of the whole space. Note that the temporal evolution of A_k is due to its elements sampled from a constant distribution per iteration. We claim that D2P2-SGD represents a unified framework over existing methods. When $p = 1$ and $A_1 = A_2 = ... = A_K = I$, D2P2-SGD degenerates to dynamically differentially private SGD (D2P-SGD) Du et al. (2021), though the original approach has another gradient clipping mechanism to prevent dynamic DPSGD from diverging and different formula for $\sigma_{\epsilon,k}^2$. On top of D2P-SGD, if we set fixed variance for ϵ_k, it becomes DPSGD without any random projection. On the other hand, PrivSGD Kasiviswanathan (2021) can also be obtained if D2P2-SGD has a fixed variance with the random projection. However, compared to PrivSGD, which involves an extra optimization to convert from the low-dimensional to high-dimensional spaces, our scheme simply uses A_k to replace the optimization, which significantly attenuates the practical implementation complexity. We also use DP2-SGD (differentially private projected SGD) to represent this case. Please see these two variants in Appendix A.2. We also remark on the additional computational overhead due to RP. A_k is regenerated per iteration by sampling from the same distribution. The total computational overhead incurred is $\mathcal{O}(dp)$. In practice, the implementation is layer-wise so the matrix multiplication is not one-shot with all parameters, mitigating the memory issue.

Algorithm 1 D2P2-SGD

1: INITIALIZE: Model parameters $\mathbf{x}_1$, step size α, number of epochs K, lower dimension p, random matrices $A_1, A_2, \ldots, A_K$, mini-batch size B, training dataset $\mathcal{D}$, noise sequence $\sigma^2_{\epsilon,1}, \sigma^2_{\epsilon,2}, \ldots, \sigma^2_{\epsilon,K}$, gradient clipping parameter γ
2: **for** $k = 1, \ldots, K$ **do**
3: Split the dataset $\mathcal{D}$ into mini-batches of size B and randomly sample one mini-batch $\mathcal{B}$
4: Compute per-sample clipped gradients: $\hat{\mathbf{g}}^s_k = \frac{\nabla f(\mathbf{x}_k;s)}{\|\nabla f(\mathbf{x}_k;s)\|+\gamma}, s \in \mathcal{B}$
5: Calculate the mini-batch stochastic gradient: $\mathbf{g}_k = \frac{1}{B}\sum_{s\sim\mathcal{B}} \hat{\mathbf{g}}^s_k$
6: Project noisy gradient using A_k: $\tilde{\mathbf{g}}_k = A_k\left(\frac{1}{\sqrt{p}}A_k^\top \mathbf{g}_k + \epsilon_k\right), \epsilon_k \sim \mathcal{N}(0, \sigma^2_{\epsilon,k}\mathbb{I}_p)$
7: Update model parameters: $\mathbf{x}_{k+1} = \mathbf{x}_k - \alpha\tilde{\mathbf{g}}_k$
8: **end for**
9: **return** $\mathbf{x}_K$

3.2 Main Results

We next show the convergence behavior for our proposed D2P2-SGD, with generally convex and non-convex objective functions, and start with assumptions. All proof is deferred to the appendix.

Assumption 1. *(a): $f(\mathbf{x})$ is smooth with modulus L for all $\mathbf{x} \in \mathbb{R}^d$ and coercive; (b) throughout the analysis, the minimum value of the objective f exists and is bounded below, i.e., $f^* := f(\mathbf{x}^*), \mathbf{x}^* = \min_{\mathbf{x}\in\mathbb{R}^d} f(\mathbf{x})$ and $f^* > -\infty$.*

Assumption 1 (a) is generic in many previous works Wang et al. (2019b); Du et al. (2021); Kasiviswanathan (2021) to imply that the variations of gradients along with optimization are bounded above by L. Many models, even including deep neural networks, can at least be approximately smooth for the corresponding losses.

Assumption 2. *The variance of stochastic gradient $\nabla f(\mathbf{x}, s)$ is bounded above by a constant $\sigma > 0$, i.e., $\mathbb{E}[\|\nabla f(\mathbf{x}, s) - \nabla f(\mathbf{x})\|] \leq \sigma^2, \forall s \in \mathcal{D}$.*

Assumption 2 is popular when analyzing the convergence behavior of SGD-type algorithms due to the mini-batch sampling. In some recent works, the bounded gradient assumption is also leveraged Zhou et al. (2020); Zhang et al. (2023), remaining a strong condition for the analysis. For example, if the objective is in a quadratic form, $f(\mathbf{x}) = \mathbf{x}^\top M\mathbf{x}$, where M is a real symmetric matrix, then $\nabla f(\mathbf{x})$ is in a linear form, which violates such an assumption. The author in Kasiviswanathan (2021) used an extra bounded second moment assumption for gradients besides the bounded variance assumption, though it is weaker than the bounded gradient assumption. In the sequel, we start the main results with the privacy guarantee.

Theorem 1. *(Privacy) Let Assumption 2 hold. There exist constants $C_1, C_2 > 0$ such that for any $\varepsilon \leq \frac{C_1 B^2 K}{n^2}$, D2P2-SGD is (ε, δ)-differentially private for any $\delta > 0$, if $\sigma^2_\epsilon \geq \frac{C_2 B^2 K^2 \ln(1/\delta)}{n^2\varepsilon^2}$.*

The detailed proof is deferred to Appendix A.3. The core idea of the proof is that at each iteration, Line 9 in Algorithm 1 post-processes the Gaussian noise mechanism that perturbs the stochastic gradient $\mathbf{g}_k$ by adding noise ϵ_k. Subsequently, the sequence of $\{\frac{1}{\sqrt{p}}A_k^\top \mathbf{g}_k + \epsilon_k\}_{k=1}^K$ is released to have privacy guarantee by following the same privacy proof of Theorem 1 in Abadi et al. (2016). However, the significant difference in our work is that the noise variance is time-varying, i.e., $\sigma^2_{\epsilon,k}$. With the explicit form of noise variance we have defined in this work, i.e., $\sigma^2_{\epsilon,k} = \frac{\sigma^2_\epsilon}{k}$, it is immediately obtained that $\sigma^2_{\epsilon,1} > \sigma^2_{\epsilon,2} > \ldots > \sigma^2_{\epsilon,K}$. In Wang et al. (2019b) and Abadi et al. (2016), the static variance has the lower bound with respect to some key constants such as K and G. Thus, as long as $\sigma^2_{\epsilon,K} \geq \frac{C_2 K B^2 \ln(1/\delta)}{n^2\epsilon^2}$, the privacy guarantee is attained. Equivalently, $\sigma^2_\epsilon \geq \frac{C_2 K^2 B^2 \ln(1/\delta)}{n^2\varepsilon^2}$ in this context. Another observation from Theorem 1 is that the size of mini-batch B has an impact on ε. When B enlarges, ε has a larger upper bound such that the model performance improves with the cost of privacy, which will be evidently validated in the result section. This also intuitively validates the fact that a larger batch typically improves deep learning model performance. Though the authors in Du et al. (2021) for the first time proposed to leverage dynamic DP mechanism to

reduce the model performance loss gap, privacy guarantee has been ensured by the dynamic power following an exponential mechanism $\sigma_{\epsilon,k} \propto \mathcal{O}(\rho^{-\frac{k}{K}})$, where ρ is a positive constant. As they still utilized the clipping mechanism from Abadi et al. (2016), they also had to establish a similar exponential mechanism for the clipping threshold, which makes their algorithm framework more complex. While in our work, thanks to the automatic clipping mechanism, there is no such requirement. We are now ready to state the results for the utility with different functions.

Theorem 2. *(Utility for convex functions) Let Assumptions 1 and 2 hold. Suppose that f is a convex function and that A is a random matrix with each element being sampled from a normal distribution $\mathcal{N}(0, \sigma_A^2)$. Also, let the additive noise of DP mechanism have the variance $\sigma_{\epsilon,k}^2$. If the step size $\alpha \leq \frac{1}{2L}$, then for the iterates $\{\mathbf{x}_k\}_{k=1}^K, K \geq 1$ generated by D2P2-SGD, the following relationship holds true*

$$\mathbb{E}[f(\bar{\mathbf{x}}_K) - f^*] \leq \frac{\|\mathbf{x}_1 - \mathbf{x}^*\|^2(1+\gamma)}{2\alpha K \sigma_A^2 \sqrt{p}} + \frac{\alpha p^{1.5}(1+\gamma)(\ln K + 1)\sigma_\epsilon^2}{2K} + \frac{\alpha p d^2 \sigma_A^2 (1+\gamma)}{2}, \tag{2}$$

where $\bar{\mathbf{x}}_K = \frac{1}{K}\sum_{k=1}^K \mathbf{x}_k$.

Theorem 2 suggests that the error bound involves three terms, the initialization error, the error of additive noise due to the DP mechanism, and the random projection approximation error. The second term implies the tradeoff between utility and privacy. If $\sigma_{\epsilon,k}^2 = \sigma_\epsilon^2$, this term becomes $(\alpha p^{1.5}(1+\gamma)\sigma_\epsilon^2)/2$, which is a constant. Instead, if $\sigma_{\epsilon,k}^2 = \frac{\sigma_\epsilon^2}{k}$, it can be bounded by $\mathcal{O}(\frac{\ln K}{K})$, which also relaxes the dependence on α to decay the magnitude. Though the model performance loss gap is reduced, dynamic variance can breach privacy. To maintain the (ε, δ)-differential privacy for D2P2-SGD, as implied in Theorem 1, the additive noise should be sampled with a larger σ_ϵ^2 to offset the privacy loss, particularly in the early phase during the optimization, compared to DPSGD. The last term is associated with model projection error, while the term $\sigma_A^2 d^2$ due to model compression can cause significant error. One empirical remedy is to leverage a small α, leading to slow convergence. Eq. 10 implies that when $K \to \infty$, D2P2-SGD converges to the neighborhood of $\mathbf{x}^*$ asymptotically with the rate of $\mathcal{O}(1/K + \ln K/K)$, up to a constant $\alpha p d^2 \sigma_A^2 (1+\gamma)/2$. Additionally, a small initialization error $\|\mathbf{x}_1 - \mathbf{x}^*\|$ and a larger batch size lead to the better performance, which stresses the implication from Theorem 1. Overall, the consolidation among complexity, utility, and privacy in D2P2-SGD is reflected explicitly in Theorem 2. The following corollary summarizes the explicit convergence rate when $\alpha = \mathcal{O}(\frac{1}{\sqrt{K}})$.

Corollary 1. *With conditions defined in Theorem 2, when $\alpha = \mathcal{O}(\frac{1}{\sqrt{K}})$, the following relationship holds true, i.e., $\mathbb{E}[f(\bar{\mathbf{x}}_K) - f^*] \leq \mathcal{O}(\frac{1}{\sqrt{K}} + \frac{\ln K}{K^{1.5}})$.*

The conclusion in Corollary 1 requires the constant learning rate α to have a format $\alpha \propto \mathcal{O}(\frac{1}{\sqrt{K}})$, which is a quite popular choice in stochastic optimization Garrigos & Gower (2023). After carefully reviewing some recent works Koloskova et al. (2023a); Bu et al. (2024); Xiao et al. (2023); Chen et al. (2020), though they have also focused on the investigation of convergence guarantee for differentially private SGD with gradient clipping, all of them paid only attention to nonconvex cases. Our result explicitly and rigorously establishes the convergence rate of D2P2-SGD for convex functions. Without dynamic differential privacy and model compression, our result resembles exactly the same convergence rate of regular SGD in $\mathcal{O}(\frac{1}{\sqrt{K}})$. Particularly, if a desired accuracy $\zeta > 0$ is defined specifically for $\mathbb{E}[f(\bar{\mathbf{x}}_K) - f^*] \leq \zeta$, the complexity bound for K is $\mathcal{O}(\frac{1}{\zeta^2} + \frac{(\ln(\frac{1}{\zeta}))^{2/3}}{\zeta^{2/3}})$. In comparison, our rate improves the one reported in Kasiviswanathan (2021), which is $\mathcal{O}(\frac{\ln K}{\sqrt{K}})$. Note that in their case, they use a decaying step size $\alpha_k \propto \frac{1}{\sqrt{k}}$ and there is no smoothness assumption. We will now present the main result for non-convex functions.

Theorem 3. *(Utility for non-convex functions) Let Assumptions 1 and 2 hold. Suppose that A is a random matrix with each element being sampled from a normal distribution $\mathcal{N}(0, \sigma_A^2)$. Also, let the additive noise of the DP mechanism have the variance $\sigma_{\epsilon,k}^2$. If the step size $\alpha \leq \frac{1}{2L}$, then for the iterates $\{\mathbf{x}_k\}_{k=1}^K, K \geq 1$ generated by D2P2-SGD, the following relationship holds true*

$$\min_{k\in[1,K]} \mathbb{E}[\|\nabla f(\mathbf{x}_k)\|] \leq \frac{f(\mathbf{x}_1) - f^*}{K\sigma_A^2\sqrt{p}\alpha} + \frac{\alpha L p^{1.5}\sigma_\epsilon^2(\ln K + 1)}{K} + L\alpha\sqrt{p}d^2\sigma_A^2 + \frac{2\sigma}{\sqrt{B}} + \gamma. \tag{3}$$

We immediately have the following result when the step size satisfies a certain condition.

Corollary 2. *With conditions defined in Theorem 3, when* $\alpha = \mathcal{O}(\frac{1}{\sqrt{K}})$*, the following relationship hold true,* $\min_{k\in[1,K]}\mathbb{E}[\|\nabla f(\mathbf{x}_k)\|] \leq \mathcal{O}(\frac{1}{\sqrt{K}} + \frac{\ln K}{K^{1.5}} + \sigma + \gamma)$.

Similarly, the error bound from Theorem 3 is dictated by the initialization error, the error of addictive noise, the random projection approximation error and the clipping bias. Especially, the clipping bias $\frac{2\sigma}{\sqrt{B}} + \gamma$ is determined by the variance, the batch size and the stability constant. To mitigate the clipping bias, one immediate solution is to properly increase the batch size. Due to γ, in practical implementation, one can choose a small value for γ. When γ is $\mathcal{O}(\frac{1}{\sqrt{K}})$ in Corollary 2, the clipping bias resembles the result in Koloskova et al. (2023a), up to some absolute constants. Also, the convergence rate of non-convex functions remains similar to that of generally convex functions. However, comparing results from Corollary 1 and Corollary 2, the error of non-convex functions is larger due to the clipping bias, which illustrates that the convergence for non-convex functions is more challenging. We summarize the clipping bias for different methods in Table 3 in Appendix A.6 for comparison (we only compare for non-convex functions as most of the existing methods only discussed non-convex objectives). Practically, non-asymptotic convergence is preferred such that we can resort to a pre-defined small constant $\xi > 0$ to define metric, i.e., the norm of gradient $\|\nabla f(\mathbf{x})\| \leq \xi$ for non-convex functions. Suppose that $B = \sigma^2/\xi^2$ and $\gamma = \mathcal{O}(\frac{1}{\sqrt{K}})$. If the computational complexity is defined as the total number of gradient computations, it can be observed that the computational complexity is $KB = \mathcal{O}(1/\xi^4)$, which retains the same complexity as in Ghadimi & Lan (2013).

4 Numerical Experiments

We present extensive empirical results to thoroughly validate our proposed approaches with the comparison to baselines. The baselines we use in this study consist of SGD, vanilla DPSGD, D2P-SGD, and DP2-SGD. D2P-SGD is an equivalent alternative to Dynamic DPSGD in Du et al. (2021). DP2-SGD can also be regarded as an equivalence of PrivSGD Kasiviswanathan (2021) since the compression technique they adopted is also random projection, with a static DP. We leverage the Opacus library Yousefpour et al. (2021) and build the framework on top of it. We use a 4-layer Convolutional Neural Network (CNN) as the model, which has been widely used in testing optimizers. A more detailed explanation of the architecture is provided in Appendix A.7. Additionally, the datasets for testing our algorithms include FashionMNIST and SVHN Figueroa (2019). As we have particularly identified the critical relationship between the privacy loss ε and other parameters, an ablation study on this is shown to reveal their impacts on the performance. Additional results on other *larger* models and datasets are in Appendix A.7.

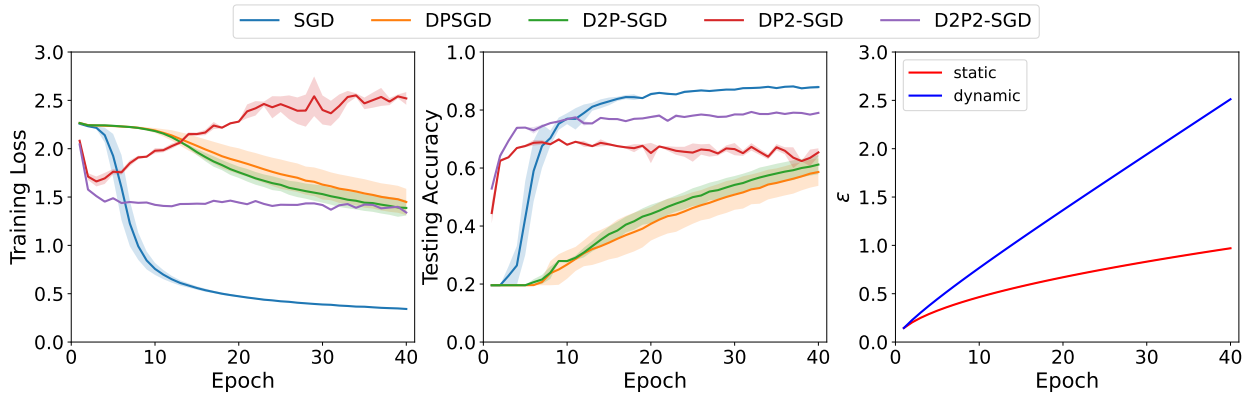

Figure 2: Comparison among methods for SVHN data: on the right side, the privacy loss is shown for static and dynamic scenarios.

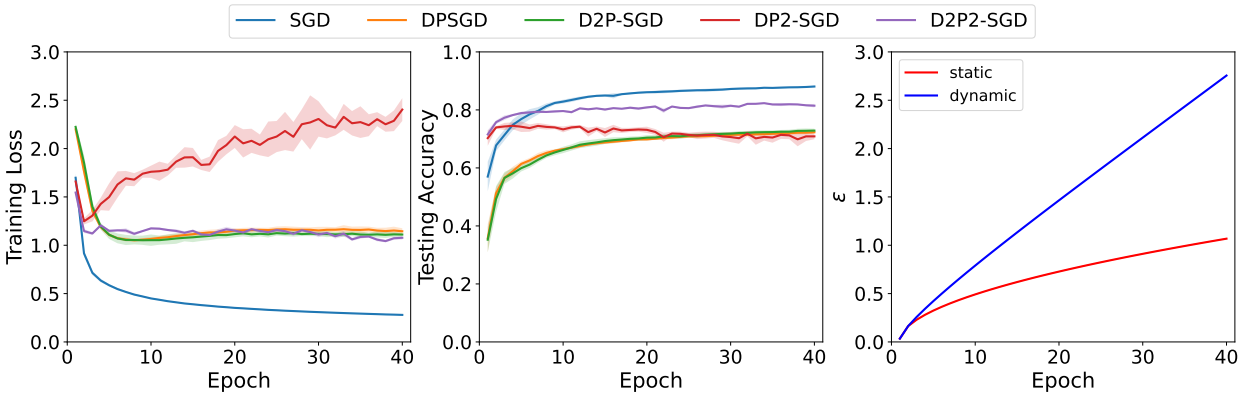

Figure 3: Comparison among methods for FashionMNIST data: on the right side, the privacy loss is shown for static and dynamic scenarios.

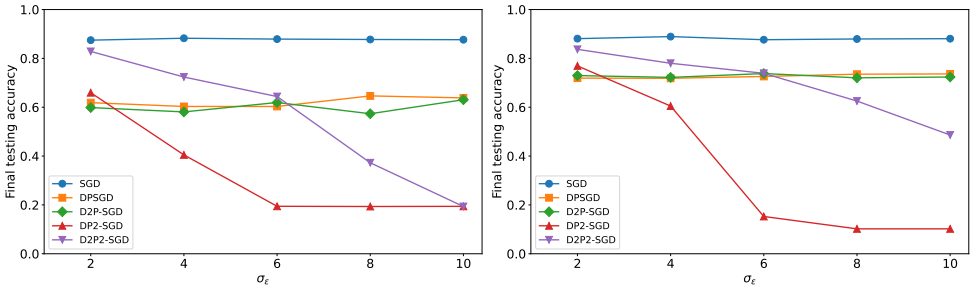

(a) SVHN (b) FashionMNIST

Figure 4: Accuracy vs. standard deviation

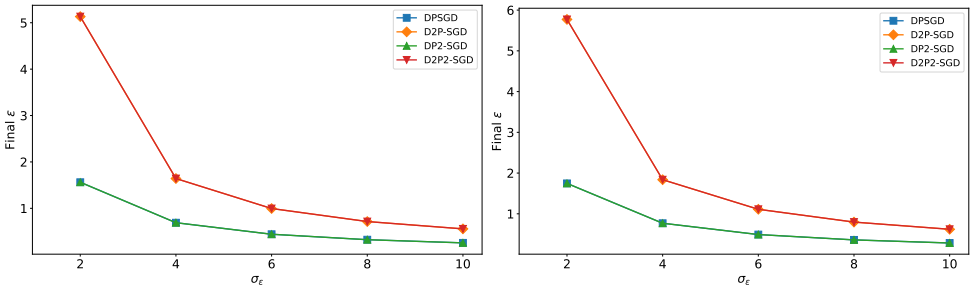

(a) SVHN (b) FashionMNIST

Figure 5: Privacy loss vs. standard deviation

Comparative Evaluation. Figure 2 shows the model performance and privacy loss for different methods. We train five different instances of each algorithm with different random seeds. The solid curves correspond to the mean and the shaded region to the minimum and maximum values over the five runs. For the privacy loss, the standard deviation is fairly small. Also, the dynamic mechanism for D2P-SGD and D2P2-SGD is the same. Similarly, DPSGD and DP2-SGD have the same static mechanism. According to Figure 2, D2P2-SGD significantly improves the model accuracy compared to DPSGD, D2P-SGD, and DP2-SGD. While this comes at the expense of a larger privacy loss, which is expected. This is attributed to the decreasing variance $\sigma_{\epsilon,k}^2/k$ along with iterations. However, the testing accuracy of D2P2-SGD is much closer to SGD, while having a gap due to projection error and clipping bias. Notably, D2P2-SGD spends a lesser number of epochs, reaching a higher accuracy at the early phase, even earlier than SGD, which implies that random projection enables more efficient model learning. The similar conclusions can be made from Figure 3. Comparing DP2-SGD and D2P2-SGD, we see that with random projection, if the noise variance from the

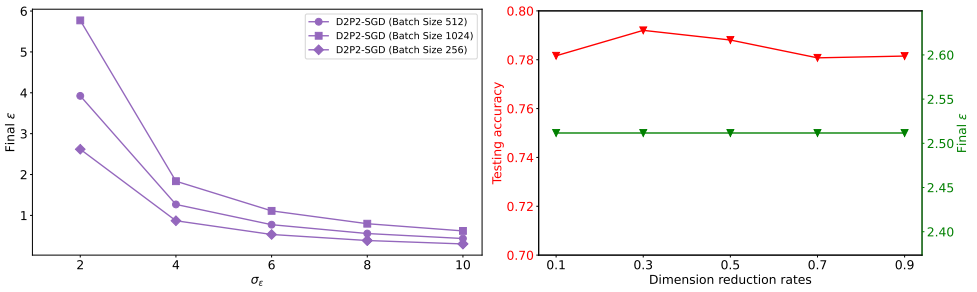

(a) Batch size vs. privacy loss for FashionMNIST

(b) Dimension vs. accuracy/privacy for SVHN

Figure 6: Impacts of parameters in D2P2-SGD

DP mechanism is static, the performance deteriorates accordingly. However, with a dynamic mechanism, it performs robustly throughout training. This validates the conclusion from Theorem 3, where the second term decays faster when the number of iterations increases. However, DP2-SGD remains with the rate of $\mathcal{O}(1/\sqrt{K})$ (If α is not in $\mathcal{O}(1/\sqrt{K})$, this term in D2P2-SGD is in $\mathcal{O}(\ln(K/K))$, while DP2-SGD $\mathcal{O}(1)$). Turning to the privacy loss (ε) in both figures, we can observe that the maximum privacy losses of the dynamic mechanism end up with respectively 2.45 (for SVHN) and 2.75 (for FashionMNIST). Compared to values with the static DP mechanism (1.06 and 0.95, respectively), the privacy loss of D2P2-SGD grows sharply. However, given the bound for ε in Theorem 1, as long as the constant C_1 (≥ 314, see Appendix A.7) is selected properly, D2P2-SGD still remains (ε, δ)-differentially private. While the value of 2.45 or 2.75 offers a reasonable, rather than exceptionally strong privacy guarantee, it reflects our focus on balancing privacy and utility. However, in highly private domains such as medical applications, D2P2-SGD can still be adopted to bias towards privacy by setting large dynamic noise. These two values are only resulting values based on the data we have applied in this work. Thus, our proposed scheme improves the accuracy over baselines while successfully maintaining differential privacy.

Impact of σ_ϵ. From Figure 4, it shows that as σ_ϵ value increases, the final model accuracy drops for DP2-SGD and D2P2-SGD. This first validates the coupling between projection error σ_A^2 and the noise variance $\sigma_{\epsilon,k}^2$ in Theorem 3 and shows the trade-off between the utility and privacy. When $\sigma_\epsilon < 6$, which can be treated as a low privacy regime, D2P2-SGD maintains better performance than DPSGD and D2P-SGD, while underperforming in the high privacy regime after $\sigma_\epsilon > 6$. This intuitively shows us a careful selection of σ_ϵ is required to balance the trade-off. Figure 5 delivers a similar conclusion in terms of privacy loss.

Impact of B. As suggested from Theorem 1, we can adjust the privacy loss by setting the batch size B. In Figure 6a, we can observe that when batch size increases from 256 to 1024, it increases the upper bound for $\varepsilon \leq \frac{C_1 B^2 K}{n^2}$ such that the privacy loss is relatively higher through all σ_ϵ for D2P2-SGD, leading to the better performance. This essentially validates the condition $B = \sigma^2/\xi^2$, where σ^2 decreases in the error bounds, leading to better convergence due to the smaller ξ.

Impact of p. Figure 6b shows the impact of different lower dimensions on the testing accuracy and privacy loss. It immediately suggests that the performance of random projection varies with different p values. The optimal one is a 30% reduction rate, which implies that random projection can assist in model learning efficiency if the p value is chosen properly. Instead, the privacy loss is independent of the dimension change based on Figure 6b. Thus, D2P2-SGD allows us to reduce the computational complexity by random projection while maintaining privacy. The dimension can be chosen in a wide range and will not affect model performance significantly, including accuracy and privacy.

Limitation. Though D2P2-SGD has shown good performance compared to the existing baselines, some potential limitations exist, which can also help us close such gaps in future work. First, D2P2-SGD may not work well in the scenarios with *high privacy restrictions*. As we have the decaying noise variance that ensures decent model performance, privacy loss will inevitably be the resulting outcome. One can carefully tune these parameters to obtain acceptable values, but it is still fairly challenging to scale. One way to get rid of this is to develop more effective dynamic DP mechanisms such that the tradeoff between utility and

privacy can be handled better. Second, getting an optimal p value for random projection may be difficult as well. Though based on Johnson-Lindenstrauss Lemma, p can be analytically obtained, its practical values for different scenarios have not yet been accessible in a principled manner.

5 Conclusions and Broader Impacts

This work presents a novel differentially private optimizer termed D2P2-SGD with dynamic DP mechanism, automatic gradient clipping, and model compression, which reveals the synthesis among privacy, utility, and complexity. Specifically, we establish the dynamic privacy guarantee such that a relatively larger variance is required in the early phase of optimization to compensate for the privacy loss in the latter phase. Given a pre-defined dynamic variance, D2P2-SGD enables a slightly tighter error bound compared to vanilla DPSGD with a static DP mechanism. Empirical results are shown to validate the theory first and then compared with baselines using popular models and benchmark datasets. Compared to vanilla DPSGD, our D2P2-SGD is more robust against larger noise variance but with a slightly larger privacy loss. However, the accuracy is significantly improved without dependence on the large dimension. The broader vision of this work is to advance the field of differentially private machine learning with the potential impact of building privacy-aware deep learning models with highly sensitive information for critical sectors such as healthcare and national security.

References

Martin Abadi, Andy Chu, Ian Goodfellow, H Brendan McMahan, Ilya Mironov, Kunal Talwar, and Li Zhang. Deep learning with differential privacy. In *Proceedings of the 2016 ACM SIGSAC conference on computer and communications security*, pp. 308–318, 2016.

Dimitris Achlioptas. Database-friendly random projections. In *Proceedings of the twentieth ACM SIGMOD-SIGACT-SIGART symposium on Principles of database systems*, pp. 274–281, 2001.

Naman Agarwal, Ananda Theertha Suresh, Felix Xinnan X Yu, Sanjiv Kumar, and Brendan McMahan. cpsgd: Communication-efficient and differentially-private distributed sgd. *Advances in Neural Information Processing Systems*, 31, 2018.

Raef Bassily, Adam Smith, and Abhradeep Thakurta. Private empirical risk minimization: Efficient algorithms and tight error bounds. In *2014 IEEE 55th annual symposium on foundations of computer science*, pp. 464–473. IEEE, 2014.

Alberto Blanco-Justicia, David Sánchez, Josep Domingo-Ferrer, and Krishnamurty Muralidhar. A critical review on the use (and misuse) of differential privacy in machine learning. *ACM Computing Surveys*, 55 (8):1–16, 2022.

Jeremiah Blocki, Avrim Blum, Anupam Datta, and Or Sheffet. The johnson-lindenstrauss transform itself preserves differential privacy. In *2012 IEEE 53rd Annual Symposium on Foundations of Computer Science*, pp. 410–419. IEEE, 2012.

Léon Bottou, Frank E Curtis, and Jorge Nocedal. Optimization methods for large-scale machine learning. *SIAM review*, 60(2):223–311, 2018.

Zhiqi Bu, Yu-Xiang Wang, Sheng Zha, and George Karypis. Automatic clipping: Differentially private deep learning made easier and stronger. *Advances in Neural Information Processing Systems*, 36, 2024.

Cristian Buciluǎ, Rich Caruana, and Alexandru Niculescu-Mizil. Model compression. In *Proceedings of the 12th ACM SIGKDD international conference on Knowledge discovery and data mining*, pp. 535–541, 2006.

Irene Y Chen, Emma Pierson, Sherri Rose, Shalmali Joshi, Kadija Ferryman, and Marzyeh Ghassemi. Ethical machine learning in healthcare. *Annual review of biomedical data science*, 4:123–144, 2021.

Xiangyi Chen, Steven Z Wu, and Mingyi Hong. Understanding gradient clipping in private sgd: A geometric perspective. *Advances in Neural Information Processing Systems*, 33:13773–13782, 2020.

Brian Chmiel, Ron Banner, Gil Shomron, Yury Nahshan, Alex Bronstein, Uri Weiser, et al. Robust quantization: One model to rule them all. *Advances in neural information processing systems*, 33:5308–5317, 2020.

Tejalal Choudhary, Vipul Mishra, Anurag Goswami, and Jagannathan Sarangapani. A comprehensive survey on model compression and acceleration. *Artificial Intelligence Review*, 53:5113–5155, 2020.

Rudrajit Das, Satyen Kale, Zheng Xu, Tong Zhang, and Sujay Sanghavi. Beyond uniform lipschitz condition in differentially private optimization. In *International Conference on Machine Learning*, pp. 7066–7101. PMLR, 2023.

Sanjoy Dasgupta, Daniel Hsu, and Nakul Verma. A concentration theorem for projections. *arXiv preprint arXiv:1206.6813*, 2012.

Jian Du, Song Li, Xiangyi Chen, Siheng Chen, and Mingyi Hong. Dynamic differential-privacy preserving sgd. *arXiv preprint arXiv:2111.00173*, 2021.

Cynthia Dwork. Differential privacy. In *International colloquium on automata, languages, and programming*, pp. 1–12. Springer, 2006.

Cynthia Dwork. Differential privacy: A survey of results. In *International conference on theory and applications of models of computation*, pp. 1–19. Springer, 2008.

Cynthia Dwork, Kunal Talwar, Abhradeep Thakurta, and Li Zhang. Analyze gauss: optimal bounds for privacy-preserving principal component analysis. In *Proceedings of the forty-sixth annual ACM symposium on Theory of computing*, pp. 11–20, 2014.

Ce Feng and Parv Venkitasubramaniam. Rqp-sgd: Differential private machine learning through noisy sgd and randomized quantization. *arXiv preprint arXiv:2402.06606*, 2024.

Jhosimar Arias Figueroa. Semi-supervised learning using deep generative models and auxiliary tasks. In *NeurIPS Workshop on Bayesian Deep Learning*, 2019.

James Flemings, Meisam Razaviyayn, and Murali Annavaram. Differentially private next-token prediction of large language models. *arXiv preprint arXiv:2403.15638*, 2024.

Guillaume Garrigos and Robert M Gower. Handbook of convergence theorems for (stochastic) gradient methods. *arXiv preprint arXiv:2301.11235*, 2023.

Saeed Ghadimi and Guanghui Lan. Stochastic first-and zeroth-order methods for nonconvex stochastic programming. *SIAM journal on optimization*, 23(4):2341–2368, 2013.

John W Goodell, Satish Kumar, Weng Marc Lim, and Debidutta Pattnaik. Artificial intelligence and machine learning in finance: Identifying foundations, themes, and research clusters from bibliometric analysis. *Journal of Behavioral and Experimental Finance*, 32:100577, 2021.

Xin Gu, Gautam Kamath, and Zhiwei Steven Wu. Choosing public datasets for private machine learning via gradient subspace distance. *arXiv preprint arXiv:2303.01256*, 2023.

Zhanglong Ji, Zachary C Lipton, and Charles Elkan. Differential privacy and machine learning: a survey and review. *arXiv preprint arXiv:1412.7584*, 2014.

Shiva Prasad Kasiviswanathan. Sgd with low-dimensional gradients with applications to private and distributed learning. In *Uncertainty in Artificial Intelligence*, pp. 1905–1915. PMLR, 2021.

Enkelejda Kasneci, Kathrin Seßler, Stefan Küchemann, Maria Bannert, Daryna Dementieva, Frank Fischer, Urs Gasser, Georg Groh, Stephan Günnemann, Eyke Hüllermeier, et al. Chatgpt for good? on opportunities and challenges of large language models for education. *Learning and individual differences*, 103: 102274, 2023.

Anastasia Koloskova, Hadrien Hendrikx, and Sebastian U Stich. Revisiting gradient clipping: Stochastic bias and tight convergence guarantees. In *International Conference on Machine Learning*, pp. 17343–17363. PMLR, 2023a.

Anastasiia Koloskova, Ryan McKenna, Zachary Charles, John Rush, and H Brendan McMahan. Gradient descent with linearly correlated noise: Theory and applications to differential privacy. *Advances in Neural Information Processing Systems*, 36, 2023b.

Kasper Green Larsen and Jelani Nelson. Optimality of the johnson-lindenstrauss lemma. In *2017 IEEE 58th Annual Symposium on Foundations of Computer Science (FOCS)*, pp. 633–638. IEEE, 2017.

Boyue Li and Yuejie Chi. Convergence and privacy of decentralized nonconvex optimization with gradient clipping and communication compression. *IEEE Journal of Selected Topics in Signal Processing*, 2025.

Justus Mattern, Zhijing Jin, Benjamin Weggenmann, Bernhard Schoelkopf, and Mrinmaya Sachan. Differentially private language models for secure data sharing. *arXiv preprint arXiv:2210.13918*, 2022.

Gaurav Menghani. Efficient deep learning: A survey on making deep learning models smaller, faster, and better. *ACM Computing Surveys*, 55(12):1–37, 2023.

Fatemehsadat Mireshghallah, Arturs Backurs, Huseyin A Inan, Lukas Wutschitz, and Janardhan Kulkarni. Differentially private model compression. *Advances in Neural Information Processing Systems*, 35:29468–29483, 2022.

Ilya Mironov. Rényi differential privacy. In *2017 IEEE 30th computer security foundations symposium (CSF)*, pp. 263–275. IEEE, 2017.

Reza Moradi, Reza Berangi, and Behrouz Minaei. A survey of regularization strategies for deep models. *Artificial Intelligence Review*, 53(6):3947–3986, 2020.

Mahmoud Nabil. Random projection and its applications. *arXiv preprint arXiv:1710.03163*, 2017.

Antonio Orvieto, Anant Raj, Hans Kersting, and Francis Bach. Explicit regularization in overparametrized models via noise injection. In *International Conference on Artificial Intelligence and Statistics*, pp. 7265–7287. PMLR, 2023.

Natalia Ponomareva, Hussein Hazimeh, Alex Kurakin, Zheng Xu, Carson Denison, H Brendan McMahan, Sergei Vassilvitskii, Steve Chien, and Abhradeep Guha Thakurta. How to dp-fy ml: A practical guide to machine learning with differential privacy. *Journal of Artificial Intelligence Research*, 77:1113–1201, 2023.

Pranav Subramani, Nicholas Vadivelu, and Gautam Kamath. Enabling fast differentially private sgd via just-in-time compilation and vectorization. *Advances in Neural Information Processing Systems*, 34:26409–26421, 2021.

Arun James Thirunavukarasu, Darren Shu Jeng Ting, Kabilan Elangovan, Laura Gutierrez, Ting Fang Tan, and Daniel Shu Wei Ting. Large language models in medicine. *Nature medicine*, 29(8):1930–1940, 2023.

Eliad Tsfadia. On differentially private subspace estimation without distributional assumptions. *arXiv preprint arXiv:2402.06465*, 2024.

Bao Wang, Zuoqiang Shi, and Stanley Osher. Resnets ensemble via the feynman-kac formalism to improve natural and robust accuracies. *Advances in Neural Information Processing Systems*, 32, 2019a.

Ji Wang, Weidong Bao, Lichao Sun, Xiaomin Zhu, Bokai Cao, and S Yu Philip. Private model compression via knowledge distillation. In *Proceedings of the AAAI Conference on Artificial Intelligence*, volume 33, pp. 1190–1197, 2019b.

Junxiao Wang, Song Guo, Xin Xie, and Heng Qi. Protect privacy from gradient leakage attack in federated learning. In *IEEE INFOCOM 2022-IEEE Conference on Computer Communications*, pp. 580–589. IEEE, 2022a.

Puyu Wang, Yunwen Lei, Yiming Ying, and Hai Zhang. Differentially private sgd with non-smooth losses. *Applied and Computational Harmonic Analysis*, 56:306–336, 2022b.

Hanshen Xiao, Zihang Xiang, Di Wang, and Srinivas Devadas. A theory to instruct differentially-private learning via clipping bias reduction. In *2023 IEEE Symposium on Security and Privacy (SP)*, pp. 2170–2189. IEEE, 2023.

Huan Xu, Constantine Caramanis, and Shie Mannor. Robust regression and lasso. *Advances in neural information processing systems*, 21, 2008.

Ashkan Yousefpour, Igor Shilov, Alexandre Sablayrolles, Davide Testuggine, Karthik Prasad, Mani Malek, John Nguyen, Sayan Ghosh, Akash Bharadwaj, Jessica Zhao, et al. Opacus: User-friendly differential privacy library in pytorch. *arXiv preprint arXiv:2109.12298*, 2021.

Da Yu, Saurabh Naik, Arturs Backurs, Sivakanth Gopi, Huseyin A Inan, Gautam Kamath, Janardhan Kulkarni, Yin Tat Lee, Andre Manoel, Lukas Wutschitz, et al. Differentially private fine-tuning of language models. *arXiv preprint arXiv:2110.06500*, 2021.

Xinwei Zhang, Zhiqi Bu, Zhiwei Steven Wu, and Mingyi Hong. Differentially private sgd without clipping bias: An error-feedback approach. *arXiv preprint arXiv:2311.14632*, 2023.

Bo Zhao, Konda Reddy Mopuri, and Hakan Bilen. idlg: Improved deep leakage from gradients. *arXiv preprint arXiv:2001.02610*, 2020.

Yingxue Zhou, Zhiwei Steven Wu, and Arindam Banerjee. Bypassing the ambient dimension: Private sgd with gradient subspace identification. *arXiv preprint arXiv:2007.03813*, 2020.

A Appendix

A.1 Additional Related Works

Beyond the works presented in the main content, differential privacy with dimension reduction has received considerable attention recently due to the emerging data-centric deep learning techniques, which require privacy-preserving yet efficient learning. Inspired by DPSGD Bassily et al. (2014), Zhou et al. Zhou et al. (2020) proposed projected DPSGD performing noise reduction by projecting the noisy gradients to a low-dimensional subspace, which is induced by the top gradient eigenspace on a small public dataset. Though PDP-SGD is theoretically and empirically validated well, the adoption of a public dataset may not be feasible in some scenarios, particularly those being data privacy-critical. Another work Mireshghallah et al. (2022) developed a technique called differentially private model compression specifically for pre-trained large language models such as GPT-2, leveraging a knowledge distillation algorithm. However, the lightweight model comes at the cost of accuracy loss. To mitigate this issue, the authors developed the differentially private iterative magnitude pruning, which produces compressed models whose performance is comparable to original models. Similarly, the author from Kasiviswanathan (2021) found that with a constraint set, SGD can be operated with the lower-dimensional (compressed) stochastic gradients, and applied it to differentially private learning with nonconvex functions to improve error bounds. However, the additive noise mechanism is still static such that the model performance gap cannot be shrunk along with iterations. In terms of differential privacy, the authors in Koloskova et al. (2023b) proposed a new stochastic optimization method that is coupled with linearly correlated noise and showed explicit convergence rates in both convex and non-convex objective functions. They also devised a new objective for the offline matrix factorization, improving the convergence property. Du et al. Du et al. (2021) presented for the first time a dynamic differentially private mechanism for SGD that can adaptively trade-off between the utility and the privacy. However, their additive noise mechanism involving an exponential function could be sophisticated to implement. A more recent work Feng & Venkitasubramaniam (2024) proposed a novel differentially private optimizer by combining noisy SGD and randomized quantization, which is close to our work. They theoretically analyzed the utility-privacy tradeoff of the proposed scheme on specifically convex losses and empirically showed results regarding the impact of different randomized quantization parameters. Unfortunately, there is no reported result on the nonconvex objectives using the developed method.

A.2 Additional Algorithms

In this section, we present additional algorithm frameworks degenerated from D2P2-SGD, including D2P-SGD (in Algorithm 2) and DP2-SGD (in Algorithm 3). We also list out the differences among these three algorithms in Table 2.

Algorithm 2 D2P-SGD

Input: Model initialization$\mathbf{x}_1$, step size α, the number of epochs K, size of mini-batch B, training set $\mathcal{D}$, noise sequence $\sigma^2_{\epsilon,1}, \sigma^2_{\epsilon,2}, ..., \sigma^2_{\epsilon,K}, \gamma$
for each k in 1 to K **do**
  Split the dataset $\mathcal{D}$ into multiple mini-batches with size B and randomly sample one $\mathcal{B}$
  Clip the per-sample gradient $\hat{\mathbf{g}}^s_k = \nabla f(\mathbf{x}_k; s)/(\|\nabla f(\mathbf{x}_k; s)\| + \gamma),\ s \in \mathcal{B}$
  Calculate the mini-batch stochastic gradient $\mathbf{g}_k = \frac{1}{B}\sum_{s\sim\mathcal{B}} \hat{\mathbf{g}}^s_k$
  Perturb the gradient $\mathbf{g}_k$ using dynamic noise: $\tilde{\mathbf{g}}_k = \mathbf{g}_k + \epsilon_k$, where $\epsilon_k \sim \mathcal{N}(0, \sigma^2_{\epsilon,k}\mathbb{I}_p)$
  Update parameter using projected noisy gradient: $\mathbf{x}_{k+1} = \mathbf{x}_k - \alpha\tilde{\mathbf{g}}_k$
end for
Output: $\mathbf{x}_K$

Algorithm 3 DP2-SGD

Input: Model initialization$\mathbf{x}_1$, step size α, the number of epochs K,lower dimension p, random matrices $A_1, A_2, ..., A_K$, size of mini-batch B, training set $\mathcal{D}$, noise variance $\sigma^2_\epsilon, \gamma$
for each k in 1 to K **do**
  Split the dataset $\mathcal{D}$ into multiple mini-batches with size B and randomly sample one $\mathcal{B}$
  Clip the per-sample gradient $\hat{\mathbf{g}}^s_k = \nabla f(\mathbf{x}_k; s)/(\|\nabla f(\mathbf{x}_k; s)\| + \gamma),\ s \in \mathcal{B}$
  Calculate the mini-batch stochastic gradient $\mathbf{g}_k = \frac{1}{B}\sum_{s\sim\mathcal{B}} \hat{\mathbf{g}}^s_k$
  Project noisy gradient using $A_k^\top$: $\tilde{\mathbf{g}}_k = A_k(\frac{1}{\sqrt{p}}A_k^\top \mathbf{g}_k + \epsilon_k)$, where $\epsilon_k \sim \mathcal{N}(0, \sigma^2_\epsilon\mathbb{I}_p)$
  Update parameter using projected noisy gradient: $\mathbf{x}_{k+1} = \mathbf{x}_k - \alpha\tilde{\mathbf{g}}_k$
end for
Output: $\mathbf{x}_K$

Table 2: D2P2-SGD and its different variants.

Method	p	$\sigma^2_{\epsilon,k}$	A_k
`D2P2-SGD`	≥ 1	$\frac{\sigma^2_\epsilon}{\sqrt{k}}$	$\mathbb{R}^{d\times p}$
`D2P-SGD`	N/A	$\frac{\sigma^2_\epsilon}{\sqrt{k}}$	$I \in \mathbb{R}^{d\times d}$
`DP2-SGD`	≥ 1	σ^2_ϵ	$\mathbb{R}^{d\times p}$

A.3 Proof for privacy guarantee

In this subsection, we provide proof of the privacy guarantee. Before that, we present some existing results to characterize the proof. We begin with a function defined in the following.

Definition 5. *Denote by $\mathcal{M}$ a randomized mechanism and by $\mathcal{D}$ and $\mathcal{D}'$ two adjacent inputs. The parameterized Rényi divergence between two distributions is defined as:*

$$\begin{aligned} e_{\mathcal{M}}(\eta) &= \sup_{\mathcal{D},\mathcal{D}'} D_\eta(\mathcal{M}(\mathcal{D})||\mathcal{M}(\mathcal{D}')) \\ &= \sup_{\mathcal{D},\mathcal{D}'} \frac{1}{\eta-1}\log\mathbb{E}_{\theta\sim\mathcal{M}(\mathcal{D}')}\left[\left(\frac{\mathcal{M}(\mathcal{D})(\theta)}{\mathcal{M}(\mathcal{D}')(\theta)}\right)^\eta\right], \end{aligned} \tag{4}$$

where $\mathcal{M}(\mathcal{D})(\theta)$ refers to the density at θ of this distribution.

With the above definition, the first result as follows is from Proposition 1 in Mironov (2017).

Lemma 1. *Let $\mathcal{M} = \mathcal{M}_K \circ \mathcal{M}_{K-1} \circ \cdots \circ \mathcal{M}_1$ be defined in an interactively compositional way, then for any fixed $\eta \geq 1$,*

$$e_{\mathcal{M}}(\eta) \leq \sum_{k=1}^{K} e_{\mathcal{M}_i}(\eta). \tag{5}$$

$e_{\mathcal{M}}(\eta)$ is defined as in Definition 5.

The K iterations of D2P2-SGD can be decomposed into K compositions of sub-sampled Gaussian mechanisms with uniform sampling without replacement. We denote by $\mathcal{G}(\sigma_\epsilon) \circ \mathcal{S}(n, B)$. With the abuse of notations, we denote by $\tilde{e}(\eta)$. the privacy-accountant functional of Eq. 4 in Definition 5. Another lemma in the following introduces a sufficient and necessary condition for a mechanism to be $(\varepsilon, \delta)-$ differentially private.

Lemma 2. *Dwork et al. (2014) Let $\mathcal{M}$ be a randomized mechanism. $\mathcal{M}$ is $(\varepsilon, \delta)-DP$ if and only if $\delta \geq \exp[(\eta - 1)(e_{\mathcal{M}}(\eta) - \varepsilon)]$, for some $\eta > 1$.*

Before the formal proof for the privacy guarantee in Theorem 1, we present another auxiliary technical lemma, which dictates the privacy amplification by uniformly sub-sampling without replacement.

Lemma 3. *For the mechanism induced by D2P2-SGD, $\mathcal{G}(\sigma_\epsilon) \circ \mathcal{S}(n, B)$, with $\frac{B}{n} < \frac{1}{10}$, the following privacy accountant holds:*

$$\tilde{e}(\eta) \leq \frac{7B^2\eta}{\sigma_\epsilon^2 n^2}, \ \forall \eta \leq \frac{\sigma_\epsilon^2}{2}\log\left(\frac{n}{B}\right). \tag{6}$$

With this in hand, we are now ready to prove Theorem 1. We restate it in the following for completeness.

Theorem 1: (Privacy) Let Assumption 2 (b) hold. There exist constants $C_1, C_2 > 0$ such that for any $\varepsilon \leq \frac{C_1 B^2 K}{n^2}$, D2P2-SGD is (ε, δ)-differentially private for any $\delta > 0$, if $\sigma_\epsilon^2 \geq \frac{C_2 B^2 K^2 \ln(1/\delta)}{n^2 \varepsilon^2}$.

Proof. With the explicit form of noise variance we have defined in this work, i.e., $\sigma_{\epsilon,k}^2 = \frac{\sigma_\epsilon^2}{k}$, it is immediately obtained that $\sigma_{\epsilon,1}^2 > \sigma_{\epsilon,2}^2 > ... > \sigma_{\epsilon,K}^2$. If $\sigma_{\epsilon,K}^2 \geq \frac{C_2 B^2 K \ln(1/\delta)}{n^2 \varepsilon^2}$, then $\sigma_{\epsilon,k}^2 \geq \frac{C_2 B^2 K \ln(1/\delta)}{n^2 \varepsilon^2}$ for all k. Thus, the core of the proof has now turned to σ_ϵ^2. As discussed before, D2P2-SGD can be treated as a composition, denoted by $\mathcal{M}$. In light of Lemma 1 and Lemma 3, it is easily obtained that

$$e_{\mathcal{M}}(\eta) \leq \frac{7K^2B^2\eta}{\sigma_\epsilon^2 n^2}, \ \forall \eta \leq \frac{\sigma_\epsilon^2}{2}\log\left(\frac{n}{B}\right). \tag{7}$$

K is due to the K iterations in D2P2-SGD and $K \leq K^2$. Additionally, based on Lemma 2, we can know that D2P2-SGD is (ε, δ)-DP is there exists $\eta \leq \frac{\sigma_\epsilon^2}{2}\log\left(\frac{n}{B}\right)$ such that

$$\frac{7K^2B^2\eta}{\sigma_\epsilon^2 n^2} \leq \varepsilon/2, \ \exp\left(\frac{-(\eta-1)\varepsilon}{2}\right) \leq \delta. \tag{8}$$

It is now easy to verify that if $\varepsilon = C_1 B^2 K^2/n^2$, all these conditions can be satisfied by setting $\sigma_\epsilon = \frac{C_2 B K \sqrt{\log(1/\delta)}}{n\varepsilon}$, for some explicit constants C_1 and C_2. □

A.4 Proof for convex objectives

A well-known result regarding the convexity is presented in the following to characterize the analysis.

Lemma 4. *(convexity Garrigos & Gower (2023)) If $f : \mathbb{R}^d \to \mathbb{R}$ is convex and differentiable, then for $\mathbf{x}, \mathbf{y} \in \mathbb{R}^d$,*

$$f(\mathbf{x}) \geq f(\mathbf{y}) + \langle \nabla f(\mathbf{y}), \mathbf{x} - \mathbf{y} \rangle \tag{9}$$

Theorem 2: (Utility for convex functions) Let Assumptions 1 and 2 hold. Suppose that f is a convex function and that A is a random matrix with each element being sampled from a normal distribution $\mathcal{N}(0, \sigma_A^2)$. Also, let the additive noise of DP mechanism have the variance $\sigma_{\epsilon,k}^2$. If the step size $\alpha \leq \frac{1}{2L}$, then for the iterates $\{\mathbf{x}_k\}_{k=1}^K, K \geq 1$ generated by D2P2-SGD, the following relationship holds true

$$\begin{aligned}\mathbb{E}[f(\bar{\mathbf{x}}_K) - f^*] \leq \frac{\|\mathbf{x}_1 - \mathbf{x}^*\|^2(G+\gamma)}{2\alpha K \sigma_A^2 \sqrt{p}} + \frac{\|\mathbf{x}_1 - \mathbf{x}^*\|\sigma}{\sqrt{B}} \\ + \frac{\alpha p^{1.5}(G+\gamma)(\ln K + 1)\sigma_\epsilon^2}{2K} + \frac{\alpha p d^2 \sigma_A^2 (G+\gamma)}{2},\end{aligned} \tag{10}$$

where $\bar{\mathbf{x}}_K = \frac{1}{K}\sum_{k=1}^K \mathbf{x}_k$.

Proof. Let $\mathbf{g}_k^s = \nabla f(\mathbf{x}_k; s)$ and define $C_s = \frac{1}{\|\mathbf{g}_k^s\|+\gamma}$. Using the update law we have:

$$\begin{aligned}
&\mathbb{E}[\|\mathbf{x}_{k+1} - \mathbf{x}^*\|^2] = \mathbb{E}[\|\mathbf{x}_k - \alpha A_k(\frac{1}{\sqrt{p}} A_k^\top \frac{1}{B}\sum_s C_s \mathbf{g}_k^s + \epsilon_k) - \mathbf{x}^*\|^2] \\
&= \mathbb{E}[\|\mathbf{x}_k - \mathbf{x}^*\|^2] + \mathbb{E}[\|\alpha A_k(\frac{1}{\sqrt{p}} A_k^\top \frac{1}{B}\sum_s C_s \mathbf{g}_k^s + \epsilon_k)\|^2] - 2\alpha\mathbb{E}[\langle \frac{1}{\sqrt{p}} A_k A_k^\top \frac{1}{B}\sum_s C_s \mathbf{g}_k^s + A_k\epsilon_k, \mathbf{x}_k - \mathbf{x}^*\rangle] \\
&= \mathbb{E}[\|\mathbf{x}_k - \mathbf{x}^*\|^2] + \mathbb{E}[\|\alpha(\frac{1}{\sqrt{p}} A_k A_k^\top \frac{1}{B}\sum_s C_s \mathbf{g}_k^s + A_k\epsilon_k)\|^2] - 2\alpha\mathbb{E}[\langle \frac{1}{\sqrt{p}}\mathbb{E}[A_k A_k^\top]\frac{\mathbf{g}_k}{\|\mathbf{g}_k\|+\gamma}, \mathbf{x}_k - \mathbf{x}^*\rangle] \\
&= \mathbb{E}[\|\mathbf{x}_k - \mathbf{x}^*\|^2] + \mathbb{E}[\|\alpha(\frac{1}{\sqrt{p}} A_k A_k^\top \frac{1}{B}\sum_s C_s \mathbf{g}_k^s + A_k\epsilon_k)\|^2] - 2\alpha\mathbb{E}[\langle \frac{1}{\sqrt{p}} p\sigma_A^2 I\frac{\mathbf{g}_k}{\|\mathbf{g}_k\|+\gamma}, \mathbf{x}_k - \mathbf{x}^*\rangle] \\
&= \mathbb{E}[\|\mathbf{x}_k - \mathbf{x}^*\|^2] + \mathbb{E}[\|\alpha(\frac{1}{\sqrt{p}} A_k A_k^\top \frac{1}{B}\sum_s C_s \mathbf{g}_k^s + A_k\epsilon_k)\|^2] - 2\alpha\sqrt{p}\sigma_A^2\mathbb{E}[\langle \mathbf{x}_k - \mathbf{x}^*, \frac{\mathbf{g}_k}{\|\mathbf{g}_k\|+\gamma}\rangle] \\
&= \mathbb{E}[\|\mathbf{x}_k - \mathbf{x}^*\|^2] + \alpha^2\mathbb{E}[\|\frac{1}{\sqrt{p}} A_k A_k^\top \frac{1}{B}\sum_s C_s \mathbf{g}_k^s\|^2] + \alpha^2\mathbb{E}[\|A_k\epsilon_k\|^2] - 2\alpha\sqrt{p}\sigma_A^2\mathbb{E}[\langle \mathbf{x}_k - \mathbf{x}^*, \frac{\mathbf{g}_k}{\|\mathbf{g}_k\|+\gamma}\rangle]
\end{aligned} \tag{11}$$

The third equality follows from that $\mathbb{E}[A_k\epsilon_k] = 0$ based on the Concentration Theorem for Projections Dasgupta et al. (2012), the independence between $A_k A_k^\top$ and $\mathbf{g}(\mathbf{x}_k)$, and $\mathbb{E}[\frac{1}{B}\sum_s C_s \mathbf{g}_k^s] = \frac{\mathbf{g}_k}{\|\mathbf{g}_k\|+\gamma}$. According to Definition 4, we know that $\mathbb{E}[A_k A_k^\top] = p\sigma_A^2 I$ Nabil (2017), which yields the fourth equality. The last equality follows similarly from $\mathbb{E}[A_k\epsilon_k] = 0$. As $\mathbb{E}[\|A_k A_k^\top\|^2] = \mathbb{E}[\left\|\sum_{i=1}^p A_{k,i}A_{k,i}^\top\right\|^2] \leq p\sum_{i=1}^p \mathbb{E}[\|A_{k,i}A_{k,i}^\top\|^2] \leq p\sum_{i=1}^p \mathbb{E}[\|A_{k,i}\|^2]\mathbb{E}[\|A_{k,i}^\top\|^2] = p^2 d^2 \sigma_A^4$. Also, $\mathbb{E}[\|A_k\epsilon_k\|^2] = \mathbb{E}[\epsilon_k^\top A_k^\top A_k\epsilon_k] = \mathbb{E}[\epsilon_k^\top \mathbb{E}[A_k^\top A_k]\epsilon_k] = \epsilon_k^\top p\sigma_A^\top I\epsilon_k = \mathbb{E}[p\sigma_A^2\|\epsilon_k\|^2]$. With $\|C_s\mathbf{g}_k^s\| \leq 1$, the following relationship holds:

$$\begin{aligned}
&\mathbb{E}[\|\mathbf{x}_{k+1} - \mathbf{x}^*\|^2] \leq \mathbb{E}[\|\mathbf{x}_k - \mathbf{x}^*\|^2] + \alpha^2 p^{1.5} d^2\sigma_A^4 + \alpha^2 p^2\sigma_A^2\sigma_{\epsilon,k}^2 - 2\alpha\sqrt{p}\sigma_A^2\mathbb{E}[\langle \mathbf{x}_k - \mathbf{x}^*, \frac{\mathbf{g}_k - \nabla f(\mathbf{x}_k) + \nabla f(\mathbf{x}_k)}{\|\mathbf{g}_k\|+\gamma}\rangle] \\
&\leq \mathbb{E}[\|\mathbf{x}_k - \mathbf{x}^*\|^2] + \alpha^2 p^{1.5} d^2\sigma_A^4 + \alpha^2 p^2\sigma_A^2\sigma_{\epsilon,k}^2 + 2\alpha\sqrt{p}\sigma_A^2\mathbb{E}[\langle \mathbf{x}^* - \mathbf{x}_k, \frac{\nabla f(\mathbf{x}_k)}{\|\mathbf{g}_k\|+\gamma}\rangle] \\
&+ 2\alpha\sqrt{p}\sigma_A^2\mathbb{E}[\langle \mathbf{x}^* - \mathbf{x}_k, \frac{\mathbf{g}_k - \nabla f(\mathbf{x}_k)}{\|\mathbf{g}_k\|+\gamma}\rangle]
\end{aligned} \tag{12}$$

As $\mathbb{E}[\mathbf{g}_k] = \nabla f(\mathbf{x}_k)$, the last term on the right hand side of the above inequality equals 0. Using Lemma 4 and Cauchy-Schwartz inequality yields the following,

$$\mathbb{E}[\|\mathbf{x}_{k+1} - \mathbf{x}^*\|^2] \leq \mathbb{E}[\|\mathbf{x}_k - \mathbf{x}^*\|^2] + \alpha^2 p^{1.5} d^2\sigma_A^4 + \alpha^2 p^2\sigma_A^2\sigma_{\epsilon,k}^2 + \frac{2\alpha\sigma_A^2\sqrt{p}}{\|\mathbf{g}_k\|+\gamma}\mathbb{E}[f^* - f(\mathbf{x}_k)] \tag{13}$$

Then, we can obtain

$$\frac{2\alpha\sigma_A^2\sqrt{p}}{\|\mathbf{g}_k\|+\gamma}\mathbb{E}[f(\mathbf{x}_k) - f^*] \leq \mathbb{E}[\|\mathbf{x}_k - \mathbf{x}^*\|^2] + \alpha^2 p^{1.5} d^2\sigma_A^4 + \alpha^2 p^2\sigma_A^2\sigma_{\epsilon,k}^2 - \mathbb{E}[\|\mathbf{x}_{k+1} - \mathbf{x}^*\|^2] \tag{14}$$

Based on the definition of the clipping mechanism, we know that $\mathbf{g} \leftarrow \mathbf{g} \cdot \frac{1}{\|\mathbf{g}\|+\gamma}$ ensures $\|\mathbf{g}_k\| \leq 1$ for all $k > 0$. Therefore, diving both sides of the last inequality by $\frac{2\alpha\sigma_A^2\sqrt{p}}{\|\mathbf{g}_k\|+\gamma}$ and applying $\|\mathbf{g}_k\| \leq 1$ produces the following

$$\begin{aligned}\mathbb{E}[f(\mathbf{x}_k) - f^*] &\leq \frac{\mathbb{E}[\|\mathbf{x}_k - \mathbf{x}^*\|^2 - \|\mathbf{x}_{k+1} - \mathbf{x}^*\|^2]}{2\sqrt{p}\sigma_A^2\alpha}(1+\gamma) + \frac{\alpha p d^2\sigma_A^2(1+\gamma)}{2} + \frac{\alpha p^{1.5}\sigma_{\epsilon,k}^2(1+\gamma)}{2} \\ &\leq \frac{\mathbb{E}[\|\mathbf{x}_k - \mathbf{x}^*\|^2 - \|\mathbf{x}_{k+1} - \mathbf{x}^*\|^2]}{2\sqrt{p}\sigma_A^2\alpha}(1+\gamma) + \frac{\alpha p d^2\sigma_A^2(1+\gamma)}{2} + \frac{\alpha p^{1.5}\sigma_{\epsilon,k}^2(1+\gamma)}{2}\end{aligned} \tag{15}$$

Summing over k from 1 to K and dividing both sides by K produces the following relationship:

$$\frac{1}{K}\sum_{k=1}^{K}\mathbb{E}[f(\mathbf{x}_k) - f^*] \leq \frac{\mathbb{E}[\|\mathbf{x}_1 - \mathbf{x}^*\|^2}{2K\alpha\sqrt{p}\sigma_A^2}(1+\gamma) + \frac{\alpha p d^2\sigma_A^2(1+\gamma)}{2} + \frac{\alpha p^{1.5}(1+\gamma)}{2K}\sum_{k=1}^{K}\sigma_{\epsilon,k}^2 \tag{16}$$

Using Jensen's inequality on $f(\mathbf{x}_k) - f^*$ (i.e., $f(\bar{\mathbf{x}}_K) - f^* \leq \frac{1}{K}\sum_{k=1}^{K}\mathbb{E}[f(\mathbf{x}_k) - f^*]$) completes the proof. □

Corollary 1. With conditions defined in Theorem 2, when $\alpha = \mathcal{O}(\frac{1}{\sqrt{K}})$, the following relationship holds true, i.e., $\mathbb{E}[f(\bar{\mathbf{x}}_K) - f^*] \leq \mathcal{O}(\frac{1}{\sqrt{K}} + \frac{\ln K}{K^{1.5}})$.

Proof. Based on the conclusion from Theorem 2, substituting $\alpha = \mathcal{O}(\frac{1}{\sqrt{K}})$ into it and applying the upper bound of the partial sum leads to the desirable result. □

A.5 Proof for non-convex objectives

In this subsection, we present the missing proof for the non-convex objectives.

Theorem 3: (Utility for non-convex functions) Let Assumptions 1 and 2 hold. Suppose that A is a random matrix with each element being sampled from a normal distribution $\mathcal{N}(0, \sigma_A^2)$. Also, let the additive noise of DP mechanism have the variance $\sigma_{\epsilon,k}^2$. If the step size $\alpha \leq \frac{1}{2L}$, and, then for the iterates $\{\mathbf{x}_k\}_{k=1}^K, K \geq 1$ generated by D2P2-SGD, the following relationship holds true

$$\min_{k\in[1,K]}\mathbb{E}[\|\nabla f(\mathbf{x}_k)\|] \leq \frac{f(\mathbf{x}_1) - f^*}{K\sigma_A^2\sqrt{p}\alpha} + \frac{\alpha L p^{1.5}\sigma_\epsilon^2(\ln K + 1)}{K} + L\alpha\sqrt{p}d^2\sigma_A^2 + 2\sigma + \gamma. \tag{17}$$

Proof. Due to the smoothness condition, we have the following relationship:

$$f(\mathbf{x}_{k+1}) \leq f(\mathbf{x}_k) + \langle\nabla f(\mathbf{x}_k), \mathbf{x}_{k+1} - \mathbf{x}_k\rangle + \frac{L}{2}\|\mathbf{x}_{k+1} - \mathbf{x}_k\|^2 \tag{18}$$

Also, we know that $(\mathbf{x}_{k+1} - \mathbf{x}_k = -\alpha A_k(\frac{1}{\sqrt{p}}A_k^\top\frac{1}{B}\sum_s C_s\mathbf{g}_k^s + \epsilon_k))$

Substituting the above equality to the smoothness equation yields the following relationship:

$$\begin{aligned}f(\mathbf{x}_{k+1}) &\leq f(\mathbf{x}_k) + \langle\nabla f(\mathbf{x}_k), -\alpha A_k(\frac{1}{\sqrt{p}}A_k^\top\frac{1}{B}\sum_s C_s\mathbf{g}_k^s + \epsilon_k)\rangle \\ &+ \frac{L\alpha^2}{2}\|A_k(\frac{1}{\sqrt{p}}A_k^\top\frac{1}{B}\sum_s C_s\mathbf{g}_k^s + \epsilon_k)\|^2\end{aligned} \tag{19}$$

Taking expectation on both sides, with the proof from Theorem 2, we can obtain the following relationships

$$\begin{aligned}
&\mathbb{E}[f(\mathbf{x}_{k+1})] \leq \mathbb{E}[f(\mathbf{x}_k)] - \alpha\mathbb{E}\left[\langle \nabla f(\mathbf{x}_k), \frac{1}{\sqrt{p}}A_k A_k^\top \frac{1}{B}\sum_s C_s \mathbf{g}_k^s + A_k\epsilon_k\rangle\right] \\
&+ \frac{L\alpha^2}{2}\mathbb{E}\left[\|\frac{1}{\sqrt{p}}A_k A_k^\top \frac{1}{B}\sum_s C_s \mathbf{g}_k^s + A_k\epsilon_k\|^2\right] \\
&\leq \mathbb{E}[f(\mathbf{x}_k)] - \alpha\mathbb{E}[\langle \nabla f(\mathbf{x}_k), \frac{1}{\sqrt{p}}A_k A_k^\top \frac{1}{B}\sum_s C_s \mathbf{g}_k^s\rangle] + \frac{L\alpha^2}{2}\mathbb{E}\left[\|\frac{1}{\sqrt{p}}A_k A_k^\top \frac{1}{B}\sum_s C_s \mathbf{g}_k^s\|^2 + \|A_k\epsilon_k\|^2\right] \\
&= \mathbb{E}[f(\mathbf{x}_k)] - \alpha\mathbb{E}[\langle \nabla f(\mathbf{x}_k), \frac{1}{\sqrt{p}}A_k A_k^\top \frac{1}{B}\sum_s C_s \mathbf{g}_k^s\rangle] + \frac{L\alpha^2}{2}\mathbb{E}\left[\|\frac{1}{\sqrt{p}}A_k A_k^\top \frac{1}{B}\sum_s C_s \mathbf{g}_k^s\|^2\right] + \frac{L\alpha^2}{2}\mathbb{E}\left[\| A_k\epsilon_k\|^2\right] \\
&= \mathbb{E}[f(\mathbf{x}_k)] - \alpha\mathbb{E}[\langle \nabla f(\mathbf{x}_k), \frac{1}{\sqrt{p}}\mathbb{E}[A_k A_k^\top]\frac{\mathbf{g}_k}{\|\mathbf{g}_k\|+\gamma}\rangle] + \frac{L\alpha^2}{2}\mathbb{E}\left[\|\frac{1}{\sqrt{p}}A_k A_k^\top \frac{1}{B}\sum_s C_s \mathbf{g}_k^s\|^2\right] + \frac{L\alpha^2}{2}\mathbb{E}\left[\| A_k\epsilon_k\|^2\right]
\end{aligned} \tag{20}$$

The second inequality is due to the expectation of $A_k\epsilon_k$ equal to 0, as shown in the generally convex case. From random projection property we know $\mathbb{E}[A_k A_k^\top] = p\sigma_A^2 I$, so we will have:

$$\begin{aligned}
&\mathbb{E}[f(\mathbf{x}_{k+1})] \leq \mathbb{E}[f(\mathbf{x}_k)] - \alpha\sqrt{p}\sigma_A^2\mathbb{E}[\langle \nabla f(\mathbf{x}_k) - \mathbf{g}_k + \mathbf{g}_k, \frac{\mathbf{g}_k}{\|\mathbf{g}_k\|+\gamma}\rangle] \\
&+ \frac{L\alpha^2}{2}\mathbb{E}\left[\|\frac{1}{\sqrt{p}}A_k A_k^\top \frac{1}{B}\sum_s C_s \mathbf{g}_k^s\|^2\right] + \frac{L\alpha^2}{2}\mathbb{E}\left[\| A_k\epsilon_k\|^2\right]
\end{aligned} \tag{21}$$

As $-\langle \mathbf{a}, \mathbf{b}\rangle \leq \|\mathbf{a}\|\|\mathbf{b}\|$ and $\mathbf{g}_k^\top \mathbf{g}_k = \|\mathbf{g}_k\|^2$, we have:

$$\begin{aligned}
&\mathbb{E}[f(\mathbf{x}_{k+1})] \leq \mathbb{E}[f(\mathbf{x}_k)] + \alpha\sqrt{p}\sigma_A^2\mathbb{E}[\|\nabla f(\mathbf{x}_k) - \mathbf{g}_k\|\frac{\|\mathbf{g}_k\|}{\|\mathbf{g}_k\|+\gamma}]\frac{L\alpha^2}{2}pd^2\sigma_A^4 + \frac{L\alpha^2}{2}p^2\sigma_A^2\sigma_{\epsilon,k}^2 - \alpha\sqrt{p}\sigma_A^2\mathbb{E}[\frac{\|\mathbf{g}_k\|+\gamma}{\|\mathbf{g}_k\|+\gamma}\|\mathbf{g}_k\|] \\
&+ \alpha\sqrt{p}\sigma_A^2\mathbb{E}[\frac{\gamma}{\|\mathbf{g}_k\|+\gamma}\|\mathbf{g}_k\|]
\end{aligned} \tag{22}$$

Since $\frac{\|\mathbf{g}_k\|}{\|\mathbf{g}_k\|+\gamma} \leq 1$, we have $\alpha\sqrt{p}\sigma_A^2\mathbb{E}[\|\nabla f(\mathbf{x}_k) - \mathbf{g}_k\|\frac{\|\mathbf{g}_k\|}{\|\mathbf{g}_k\|+\gamma}] \leq \alpha\sqrt{p}\sigma_A^2\mathbb{E}[\|\nabla f(\mathbf{x}_k) - \mathbf{g}_k\|]$. Hence, with $\|\nabla f(\mathbf{x}_k)\| \leq \|\nabla f(\mathbf{x}_k) - \mathbf{g}_k\| + \|\mathbf{g}_k\|$ the following relationship can be obtained:

$$\begin{aligned}
&\alpha\sqrt{p}\sigma_A^2\mathbb{E}[\|\nabla f(\mathbf{x}_k)\|] \leq \mathbb{E}[f(\mathbf{x}_k) - f(\mathbf{x}_{k+1})] + 2\alpha\sqrt{p}\sigma_A^2\mathbb{E}[\|\nabla f(\mathbf{x}_k) - \mathbf{g}_k\|] \\
&+ \frac{L\alpha^2}{2}pd^2\sigma_A^4 + \frac{L\alpha^2}{2}p^2\sigma_A^2\sigma_{\epsilon,k}^2 + \alpha\sqrt{p}\sigma_A^2\mathbb{E}[\frac{\gamma}{\|\mathbf{g}_k\|+\gamma}\|\mathbf{g}_k\|]
\end{aligned} \tag{23}$$

Dividing both sides of the last inequality by $\alpha\sqrt{p}\sigma_A^2$ yields:

$$\begin{aligned}
&\mathbb{E}[\|\nabla f(\mathbf{x}_k)\|] \leq \frac{\mathbb{E}[f(\mathbf{x}_k) - f(\mathbf{x}_{k+1})]}{\alpha\sqrt{p}\sigma_A^2} + 2\mathbb{E}[\|\nabla f(\mathbf{x}_k) - \mathbf{g}_k\|] \\
&+ \frac{L\alpha\sqrt{p}d^2\sigma_A^2}{2} + \frac{L\alpha p^{1.5}\sigma_{\epsilon,k}^2}{2} + \gamma
\end{aligned} \tag{24}$$

which is due to $\frac{\gamma}{\|\mathbf{g}_k\|+\gamma}\|\mathbf{g}_k\| \leq \gamma$. Since $\mathbb{E}[\|\nabla f(\mathbf{x}_k) - \mathbf{g}_k\|] \leq \sqrt{\mathbb{E}[\|\nabla f(\mathbf{x}_k) - \mathbf{g}_k\|^2]} \leq \frac{\sigma}{\sqrt{B}}$ Summing the last equation over from 1 to K and dividing both sides by K grants us the following relationship:

$$\frac{1}{K}\sum_{k=1}^{K}\mathbb{E}[\|\nabla f(\mathbf{x}_k)\|] \leq \frac{f(\mathbf{x}_1)}{\alpha\sigma_A^2\sqrt{p}K} + 2\frac{\sigma}{\sqrt{B}} + \gamma + \frac{L\alpha\sqrt{p}d^2\sigma_A^2}{2} + \frac{L\alpha p^{1.5}}{2K}\sum_{k=1}^{K}\sigma_{\epsilon,k}^2 \tag{25}$$

With the fact that $\sum_{k=1}^{K}\sigma_{\epsilon,k}^2 \leq (\ln K + 1)\sigma_\epsilon^2$ and that the minimum is less than the average, the desirable result is obtained. □

Corollary 2. With conditions defined in Theorem 3, when $\alpha = \mathcal{O}(\frac{1}{\sqrt{K}})$, the following relationship hold true, $\min_{k\in[1,K]}\mathbb{E}[\|\nabla f(\mathbf{x}_k)\|] \leq \mathcal{O}(\frac{1}{\sqrt{K}} + \frac{\ln K}{K^{1.5}} + \sigma + \gamma)$.

Proof. Using the conclusion from Theorem 3 and substituting the step size α into the conclusion yields the desirable result. □

A.6 Comparison of the Clipping Bias

In this subsection, we show the comparison among different methods for the clipping bias in Table 3. It suggests that our clipping bias is proportional to σ, which is the same as in existing works. However, due to the adoption of per-sample gradient normalization, the stability constant γ also affects the clipping bias. In practice, γ is a small positive constant similar to the one in the Adam optimizer.

Table 3: Comparison among different methods.

Method	**Clipping Bias**
Chen et al. (2020)	Wasserstein distance
Koloskova et al. (2023a)	σ or σ^2/a
Xiao et al. (2023)	15σ
Bu et al. (2024)	σ/r
`D2P2-SGD (Ours)`	$2\sigma/\sqrt{B} + \gamma$

$a > 0$ is the clipping threshold; $r > 0$

A.7 Additional Results

All the experiments were conducted on a machine equipped with an Intel Xeon Silver 4110 CPU and an NVIDIA Titan RTX GPU.

A.7.1 Additional Datasets

Figure 7 shows the performance with ResNet20 Wang et al. (2019a) on the CIFAR-10 dataset. From the plots, we can observe that D2P-SGD slightly performs better than D2P2-SGD due to the random projection error in the error bound, which also deteriorates the performance of DP2-SGD. The dynamic variance mechanism plays a central role in enhancing performance closer to SGD. However, the tradeoff between random projection and privacy drives the performance of D2P2-SGD between those in D2P-SGD (upper) and DP2-SGD (lower).

In Figures 8 and 9, results for the CIFAR-10 dataset are provided, showing a similar trend to the other datasets. We also compare them to disclose the impact of the reduction rate. The reduction rate is the number of dimensions that have been compressed in random projection. For example, if $d = 10000$ and the reduction rate is 0.3, then $p = 7000$. The chosen hyperparameters are: batch size = 1024, $\sigma_\epsilon = 2.0$, and dimension reduction rate = 0.3 in Figure 8. If we decrease the dimension reduction rate to 0.1 in Figure 9, we can observe that the performance is enhanced, but the privacy loss remains the same, which aligns with our findings in the main contents.

In Figure 10, when reducing $\sigma_\epsilon = 1.0$, we can see a significant accuracy improvement, but with a sacrifice of privacy loss instead. However, D2P2-SGD achieves the best performance over baselines and is favorably comparable to SGD. Similarly, for Figures 11-13 (KMNIST, EMNIST, MNIST), D2P2-SGD is favorably comparable to or outperform all baselines, which strengthens our claims.

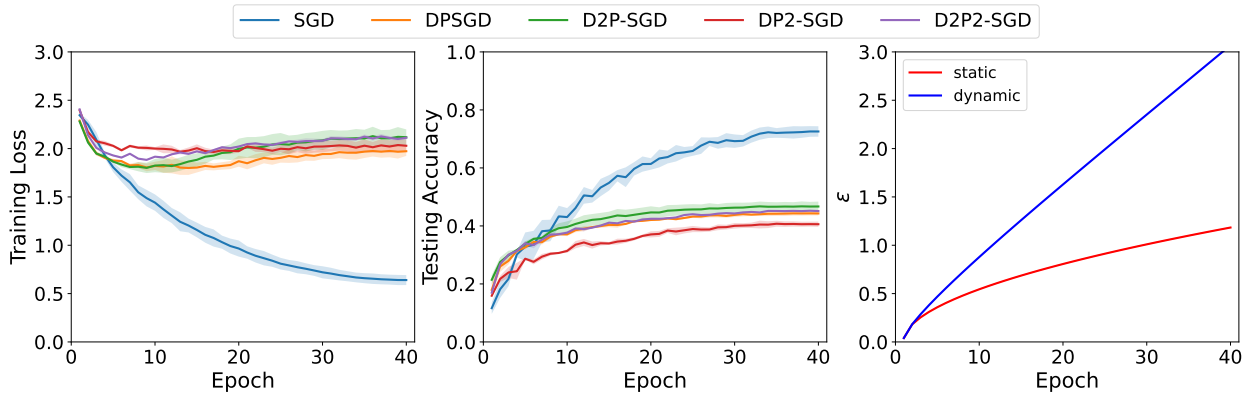

Figure 7: Comparison among different methods for CIFAR10 data with ResNet20: on the right side, the privacy loss is shown for static and dynamic scenarios.

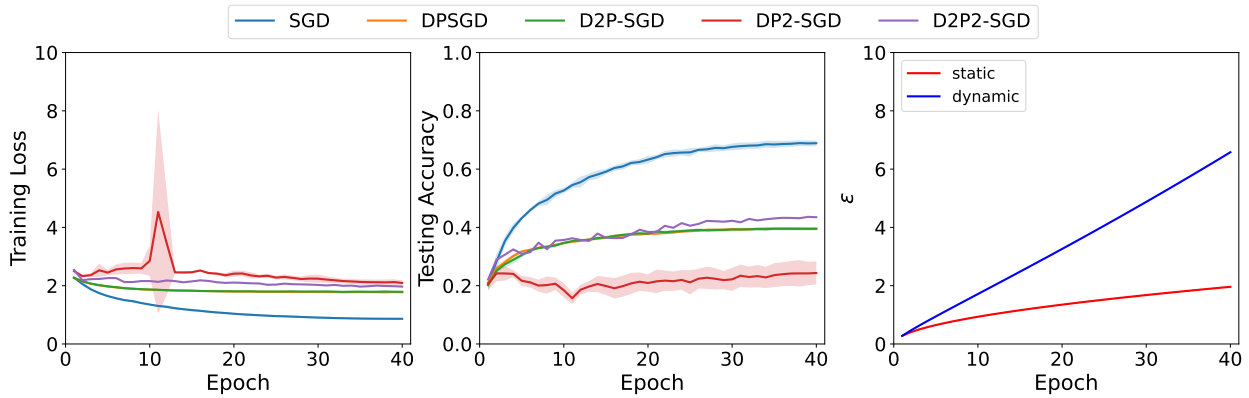

Figure 8: Comparison among different methods for CIFAR10 data with reduction rate being 0.3, with CNN: on the right side, the privacy loss is shown for static and dynamic scenarios.

A.7.2 Calculation of C_1 value

From Figures 2 and 3, given the batch size equal to 1024, the number of epoch 40, and the training data sizes 60000 and 73257, based on the upper bound for ε in Theorem 1, $\varepsilon \leq \frac{C_1 B^2 K}{n^2}$, we can obtain that as long as $C_1 \geq 314$, ε values for both datasets will remain within the bound.

A.7.3 Detail of network architecture

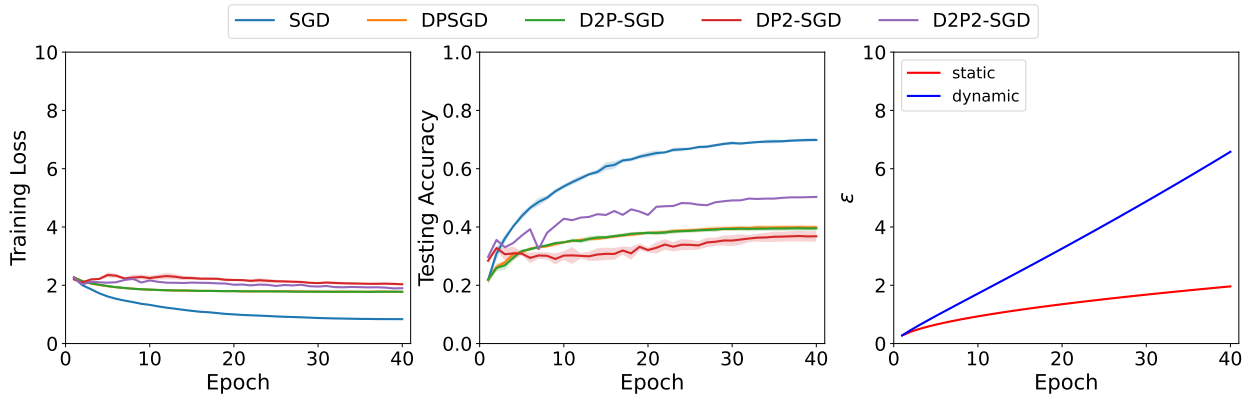

Figure 9: Comparison among different methods for CIFAR10 data with reduction rate being 0.1, with CNN: on the right side, the privacy loss is shown for static and dynamic scenarios.

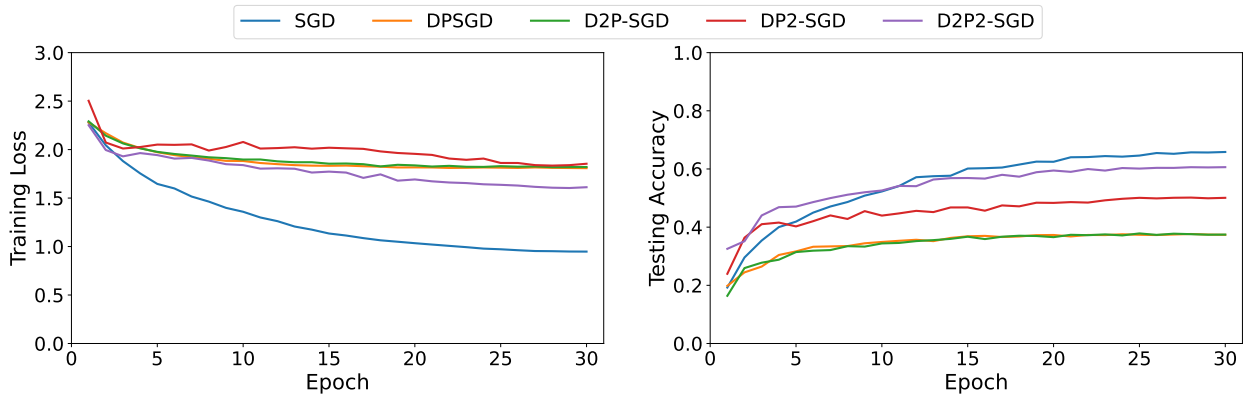

Figure 10: Comparison among different methods for CIFAR10 data with CNN: training loss and testing accuracy.

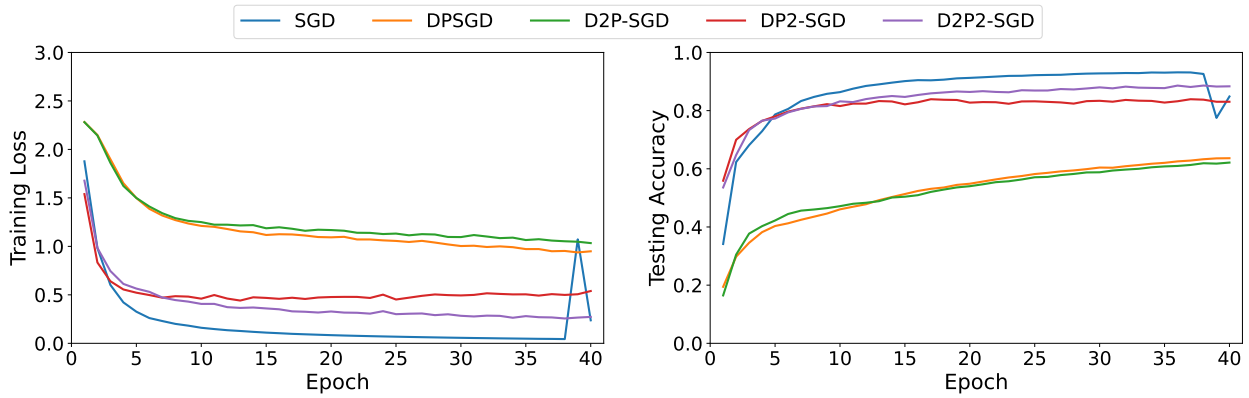

Figure 11: Comparison among different methods for KMNIST data with CNN: training loss and testing accuracy.

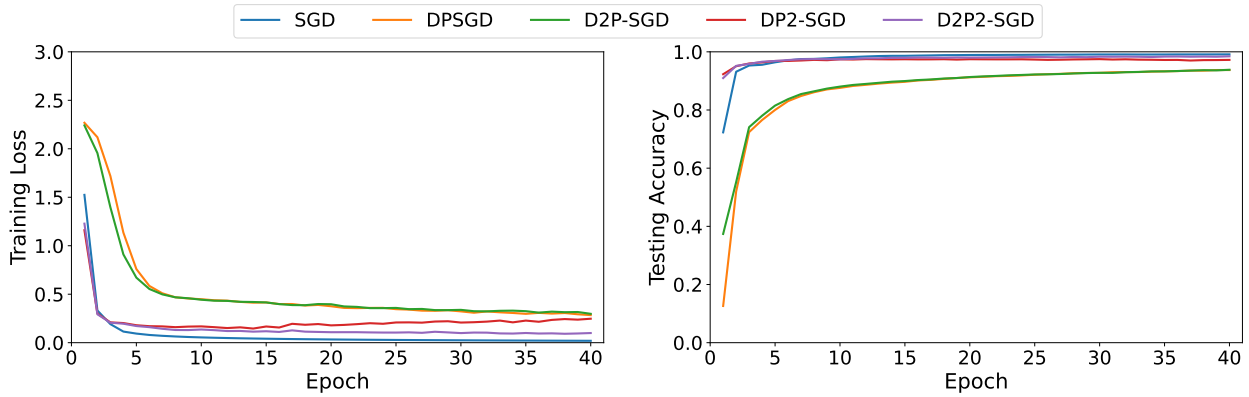

Figure 12: Comparison among different methods for EMNIST data with CNN: training loss and testing accuracy.

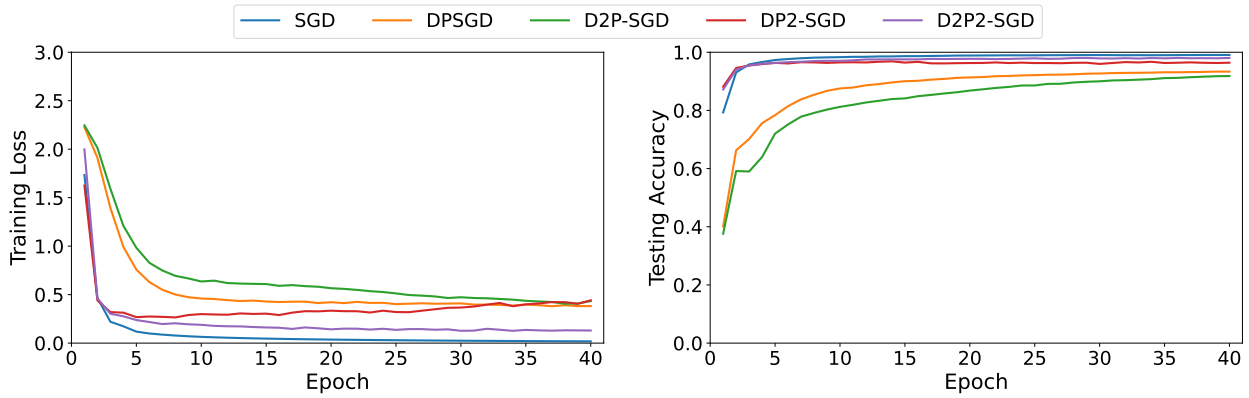

Figure 13: Comparison among different methods for MNIST data with CNN: training loss and testing accuracy.

Table 4: Network architecture for FashionMNIST, SVHN, and CIFAR-10 datasets.

Layer	**Parameters**
Convolution	16 filters of 3×3, strides 1
Average Pooling	2×2
Convolution	32 filters of 3×3, strides 1
Average Pooling	2×2
Convolution	32 filters of 3×3, strides 1
Average Pooling	2×2
Convolution	64 filters of 3×3, strides 1
Adaptive Average Pooling	1×1
Fully connected	64 units
Softmax	10 units